 doi:10.1111/mmi.12648

Probing druggability and biological function of essential proteins in *Leishmania* combining facilitated null mutant and plasmid shuffle analyses

Mariko Dacher,[1] Miguel A. Morales,[1†] Pascale Pescher,[1] Olivier Leclercq,[1] Najma Rachidi,[1] Eric Prina,[1] Mathieu Cayla,[1] Albert Descoteaux[2] and Gerald F. Späth[1*]

[1]*Institut Pasteur, CNRS URA 2581, Unité de Parasitologie moléculaire et Signalisation, Paris, France.*
[2]*INRS-Institut Armand-Frappier and Center for Host-Parasite Interactions, Laval, Québec, Canada.*

Summary

***Leishmania* parasites cause important human morbidity and mortality. Essential *Leishmania* genes escape genetic assessment by loss-of-function analyses due to lethal null mutant phenotypes, even though these genes and their products are biologically most significant and represent validated drug targets. Here we overcome this limitation using a facilitated null mutant approach applied for the functional genetic analysis of the MAP kinase LmaMPK4. This system relies on the episomal expression of the target gene from vector pXNG that expresses the *Herpes simplex* virus thymidine kinase gene thus rendering transgenic parasites susceptible for negative selection using the antiviral drug ganciclovir. Using this system we establish the genetic proof of LmaMPK4 as essential kinase in promastigotes. LmaMPK4 structure/function analysis by plasmid shuffle allowed us to identify regulatory kinase sequence elements relevant for chemotherapeutic intervention. A partial null mutant, expressing an MPK4 derivative with altered ATP-binding properties, showed defects in metacyclogenesis, establishing a first link of MPK4 function to parasite differentiation. The approaches presented here are broadly applicable to any essential gene in *Leishmania* thus overcoming major bottlenecks for their functional genetic analysis and their exploitation for structure-informed drug development.**

Accepted 9 May, 2014. *For correspondence. E-mail gspaeth@pasteur.fr; Tel. (+33) 1 40 61 38 58; Fax (+33) 1 45 68 83 32. †Present address: Department of Biological Sciences, University of Notre Dame, Notre Dame, IN 4655, USA.

Introduction

Trypanosomatid parasites of the genus *Leishmania* generate severe morbidity and mortality around the world causing a spectrum of immunopathological diseases, which include cutaneous, muco-cutaneous and visceral leishmaniasis (Desjeux, 2004). The lack of vaccines, the toxicity and costs of current anti-leishmanial therapies, and the rise of drug-resistant parasites urgently call for the development of safe and affordable new treatment options (Croft and Coombs, 2003). Several co-ordinated efforts currently utilize phenotypic and target-based strategies to identify novel compounds that interfere with essential *Leishmania*-specific pathways, including signalling processes that govern parasite stage differentiation and that are essential for intracellular infection (Dujardin *et al*., 2010).

Leishmania undergoes various differentiation steps during its life cycle that are induced by host environmental signals and that adapt the parasite for extra- and intracellular survival and proliferation. Flagellated promastigote parasites develop inside the digestive tract of phlebotomine sand flies at neutral pH and moderate temperatures at around 25°C. Proliferating procyclic promastigotes eventually differentiate into needle-shaped, cell cycle-arrested metacyclic promastigotes in response to nutritional starvation or acidification (Sacks and Perkins, 1984; Zakai *et al*., 1998; Cunningham *et al*., 2001). This form of the parasite is highly infectious and is inoculated into vertebrate hosts, including humans, during the blood meal of infected sand flies. Following transmission, parasites are ingested by phagocytes of the endo-reticular system, including macrophages, where they develop into the non-motile amastigote form in response to pH and temperature changes encountered inside the host cell phago-lysosome (Zilberstein and Shapira, 1994). Evasion and modulation of host cell immune functions by intracellular amastigotes ultimately cause the pathologies of all forms of leishmaniasis. Conceivably, signalling pathways that govern

environmentally induced amastigote differentiation and intracellular survival represent interesting new targets for anti-leishmanial chemotherapy. One such pathway is represented by signalling cascades involving extracellular-regulated mitogen-activated protein kinases (MAPKs).

MAPKs are protein kinases that are activated in response to various environmental signals, including pH, temperature, nutritional stress, hormones, or cell-to-cell and substrate-to-cell contacts, through dual phosphorylation on a highly conserved TXY motif inside the kinase activation loop (Chang and Karin, 2001; Roskoski, 2012). MAPK phosphorylation occurs by upstream MAPK kinases (M2Ks) that in turn are activated by phosphorylation through M3Ks. This signalling cascade ultimately adapts the cellular phenotype to environmental changes through transcriptional regulation and differential gene expression. Although this cascade is conserved in *Leishmania* (Pearson *et al*., 2001; Wiese, 2007), the functions of parasite MAPKs in stage differentiation and their downstream targets are only poorly elucidated.

Genetic analyses of *Leishmania major* MAPKs (termed LmaMPKs) by transgenic approaches revealed amastigote-specific phosphorylation and activity of LmaMPK4, 7 and 10 (Morales *et al*., 2007), and established a role of LmaMPK7 in translational control of amastigote proliferation (Morales *et al*., 2010a). Null mutant analysis of *Leishmania mexicana* MAPKs (termed LmxMPKs) implicated LmxMPK3 and LmxMPK9 in flagellar length control (Bengs *et al*., 2005; Erdmann *et al*., 2006), and showed the requirement of LmxMPK1 for intracellular parasite survival (Wiese, 1998). However, many members of the *Leishmania* MAP kinase pathway and of other protein kinase families escape loss-of-function analysis due to their essential nature, which either results in a lethal null mutant phenotype, or causes compensatory genetic or regulatory responses. For example, disruption of both alleles of the *L. mexicana* Cdc2-Related Kinases crk1 and crk3, and of the *L. major* MEKK-related kinase MRK1 caused changes in cell ploidy likely to avoid deletion of these putative essential genes (Mottram *et al*., 1996; Hassan *et al*., 2001; Agron *et al*., 2005). Null mutants of the *L. mexicana* MAPKs LmxMPK4 and LmxMPK6 have been suggested to be essential based on the observations that respective null mutants could only be generated in the presence of an episome expressing the target gene (Wang *et al*., 2005; Wiese *et al*., 2009). However, this approach in itself does not provide the genetic proof of essentiality of a given gene as transgene expression may simply facilitate parasite survival during genetic manipulation and selection. Likewise, maintenance of the episome in absence of selection for the respective antibiotic resistance marker has been used as readout for essentiality, yet transgene expression may just provide an advantage for *in vivo* and *in vitro* growth thus selecting for episome persistence. Finally, this approach neither allows for genetic analysis of biological functions, nor allows for structure/function analyses based on mutagenesis and genetic complementation, which could inform on kinase residues or domains relevant for drug development. Thus the absence of inducible expression systems in *Leishmania* required for conditional null mutant analysis strongly compromises our insight into the function of essential protein kinases or any essential parasite gene, even though these genes and their products are biologically most significant and represent validated drug targets.

Here we used a facilitated knockout approach based on transgenic expression of the target gene from vector pXNG that carries an expression cassette for the *Herpes simplex* virus thymidine kinase (*HSV*-TK), which allows for negative selection against this plasmid using the anti-viral drug ganciclovir (GCV) (Murta *et al*., 2009). We applied this approach on the genetic analysis of *L. major* MPK4 and established the definitive proof of the essential nature of LmaMPK4 in promastigotes based on the persistence of the pXNG-MPK4 episome in facilitated null mutants despite negative selection. We were able to functionally probe parasite-specific MPK4 sequence elements and regulatory residues by expressing various kinase mutants from a second episome and analysing their capacity to allow removal of pXNG-MPK4 by plasmid shuffle during negative selection (Morales *et al*., 2010b). Finally, we applied this approach to establish a partial MPK4 knockout expressing an LmaMPK4 mutant with altered ATP-binding properties that allowed us to uncover a first link of this protein kinase to pH-sensing and metacyclic differentiation.

Results

Establishment of a facilitated L. major *LmaMPK4 null mutant*

The genetics analysis of *Leishmania* signalling proteins by loss-of-function approaches are often rendered impossible by the essential nature of the respective genes that causes a lethal null mutant phenotype. This is for example illustrated by null mutant analyses of highly conserved *Leishmania* protein kinases, which have been suggested to be essential based on the observation that null mutants could only be obtained in transgenic parasites expressing the target gene from an episomal vector (Mottram *et al*., 1996; Hassan *et al*., 2001; Agron *et al*., 2005; Wang *et al*., 2005; Wiese *et al*., 2009). Here we applied a novel facilitated null mutant approach to study LmaMPK4 with the aim to establish the formal genetic proof of its essential nature in *L. major* by negative selection, and to gain new insight into parasite-specific structural elements and LmaMPK4 biological functions.

Transgenic parasites were established expressing a wild-type copy of LmaMPK4 from the vector pXNG (referred to as *mpk4+/+*[pXNGK4]). This vector carries expression cassettes for the *Herpes simplex* virus thymidine kinase (*HSV*-TK) and for GFP, which allows for negative selection against this plasmid using the antiviral drug ganciclovir (GCV), and for monitoring the presence of this plasmid by FACS analysis respectively (Fig. 1A) (Murta *et al*., 2009). Independent null mutant clones were established by sequential electroporation and selection using two targeting constructs comprising hygromycin B (HYG) and puromycin (PAC) resistance cassettes flanked by 900 bp of the LmaMPK4 5′ and 3′ untranslated regions (UTR). In total 10 independent clones were obtained and three independent homozygous null mutant clones (clones 3, 5 and 7) were identified by PCR analysis using genomic DNA and primer pairs diagnostic for (i) correct chromosomal integration of the two resistance cassettes (primer p1 in combination with p2 and p3, Fig. 1A and B upper panel, only clones 3 and 5 are shown), (ii) loss of the endogenous LmaMPK4 ORFs (p4 and p5, Fig. 1B, lower panel), and (iii) presence of pXNGK4 (p6 and p7, Fig. 1B, lower panel). Together these data document the establishment of independent facilitated LmaMPK4 knockout lines. For subsequent in-depth analysis, we selected the two independent clones 3 and 5.

We first investigated whether expression of pXNGK4 alone can fully compensate for the absence of endogenous MPK4 in the facilitated null mutant clones 3 and 5. Both *mpk4–/–*[pXNGK4] clones and a wild-type control transfected with pXNGK4 (termed *mpk4+/+*[pXNGK4]) were similar to untransfected parasites with respect to morphology (data not shown), *in vitro* growth (Fig. 1C) and intracellular survival in peritoneal macrophages (Fig. 1D). To investigate the effect of MPK4 expression on parasite infectivity, mouse footpad infection was performed using the *mpk4+/+*[pXNGK4] control pool and both *mpk4–/–*[pXNGK4] clones. All cells were passaged once before through mice to normalize for differences in *in vitro* passage number that may affect infectivity in a non-specific manner (data not shown). For virulence assessment, 5×10^5 stationary-phase parasites were inoculated into the hind footpads of five female BALB/c mice per group, and the size of the lesion was measured weekly over a 9-week period by comparing the thickness of infected to non-infected footpads. Neither *mpk4+/+*[pXNGK4] nor *mpk4–/–*[pXNGK4] parasites showed any significant difference in their capacity to elicit cutaneous lesions when compared to non-transfected parasites, even though the *mpk4–/–*[pXNGK4] null mutant clones showed a slight but statistically insignificant delay in lesion formation (Fig. 1E). After 9 weeks, *mpk4+/+*[pXNGK4] and *mpk4–/–*[pXNGK4] parasites were recovered from the lesions of two of the infected mice by aspiration and cultured in the absence of selective drug. As judged by FACS quantification of GFP fluorescence after conversion into promastigotes, pXNGK4 persisted in WT parasites, albeit at lower levels compared to the initial inoculum (Fig. 1F, left panel), suggesting passive loss of the episome during the course of infection. In contrast, compared to the original parasite population before inoculation, *mpk4–/–*[pXNGK4] null mutants showed significantly enhanced GFP fluorescence levels suggesting episomal amplification *in vivo* (Fig. 1F, right panel). Together our results demonstrate that the MPK4 facilitated null mutants retain normal infectivity and that pXNGK4 is amplified in these mutants during *in vivo* infection, which indicates important roles of *L. major* MPK4 in amastigote virulence similar to previous observations published in *L. mexicana* (Wang *et al*., 2005).

LmaMPK4 is essential for promastigote viability in vitro

We tested if the episomal copy of MPK4 expressed from pXNGK4 is essential for the null mutants by negative selection. Parasite culture medium containing 250 μg ml^{-1} of nourseothricin was replaced with medium supplemented with 50 μg ml^{-1} of GCV. This pro-drug is used as substrate by the *Herpes simplex* virus thymidine kinase (*HSV*-TK) expressed from pXNG, which is subsequently further phosphorylated by endogenous kinases yielding GCV-triphosphate (GCV-TP), a toxic guanosine analogue that can cause premature termination of DNA synthesis and cellular stress. In presence of GCV, the parasite thus favours elimination of the episome to avoid toxicity (Murta *et al*., 2009). We first evaluated pXNGK4 levels at passage three comparing GFP fluorescence levels of the *mpk4+/+*[pXNGK4] control pool and the two independent *mpk4–/–*[pXNGK4] null mutant clones 3 and 5 in the presence of NTC (positive selection; Fig. 2A upper panel) or GCV (negative selection; Fig. 2A lower panel) by GFP FACS analysis. The fraction of *mpk4+/+*[pXNGK4] parasites with high GFP fluorescence levels showed a reduction from 93.1% to 14% in the presence of GCV, documenting efficient loss of pXNGK4 as a result of negative selection (Fig. 2A). In contrast, high GFP fluorescence levels persisted in *mpk4–/–*[pXNGK4] clone 3 and 5 (77% and 74% respectively), despite the toxic effect of GCV-TP due to the essential nature of MPK4 expressed from pXNG.

We next investigated the kinetics of episome loss during five passages of GCV treatment using mean GFP fluorescence levels (relative FI) as readout. In the absence of nourseothricin, both *mpk4+/+*[pXNG] and *mpk4+/+*[pXNGK4] control parasites showed a robust loss of episome after the first passage with a reduction in relative FI of respectively 63% and 40% without GCV, and 78% and 50% with GCV (Fig. 2B). At passage 3, for both

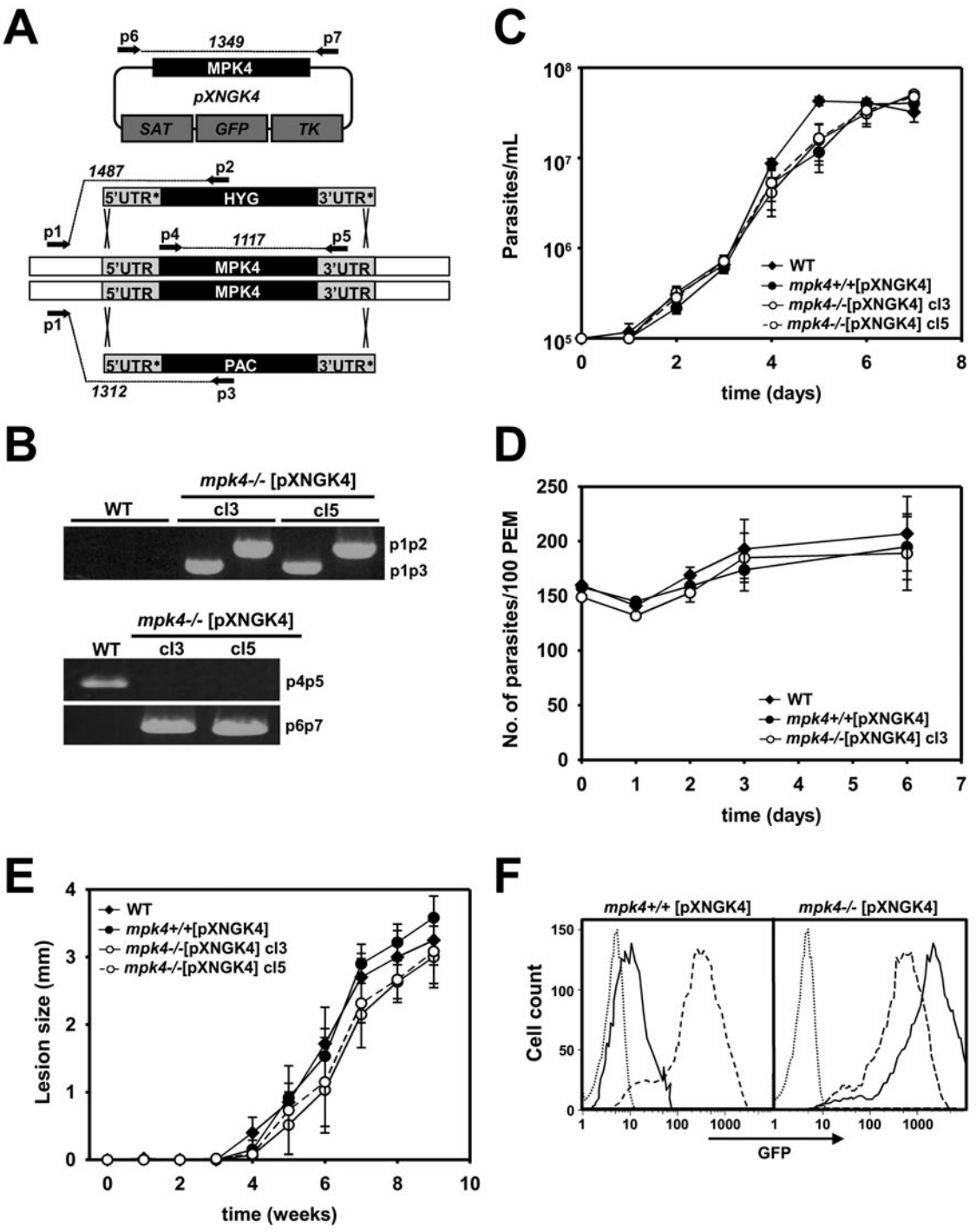

control lines, the reduction in relative FI in GCV treated parasites was significantly stronger (95% and 90% respectively) compared to untreated control (70% for both), demonstrating that active loss through negative selection is more efficient than passive loss through cell division (Fig. 2B). In contrast to the controls, *mpk4–/–*[pXNGK4] parasites maintained the episome at high levels in absence of selection, which indicates a requirement of MPK4 for *in vitro* growth or its essential function in parasite viability. We genetically tested these possibilities by negative selection: the episome persisted in the facilitated null mutant even in the presence of toxic GCV with a reduction of 10% and 23% at day 1 and day 5 of treatment respectively. Together these data provide evidence that MPK4 does not just provide a selective growth advantage but carries essential functions for parasite viability.

Fig. 1. Establishment of *L. major* MPK4 facilitated knockout parasites.
A. Schematic representation of the KO strategy. The two alleles of MPK4 were replaced by hygromycin (HYG) and puromycin (PAC) resistance cassettes in the presence of the episomal vector pXNG carrying the LmaMPK4 wild-type ORF (pXNGK4) yielding homozygous facilitated null mutant *mpk4–/–*[pXNGK4]. GFP, green fluorescent protein; SAT, streptothrycin acetyl-transferase that confers resistance against nourseothricin; TK, *Herpes simplex* virus thymidine kinase; 5′UTR, 5′ untranslated region; 3′UTR, 3′ untranslated region. The pairs of oligonucleotides used for PCR amplifications (p_xp_y) and the predicted sizes of the PCR products in bp are indicated.
B. PCR validation of gene deletion. PCR reactions specific for the inserted resistance cassettes (upper panel) and endogenous or episomal LmaMPK4 ORFs (lower panel) were performed.
C. *In vitro* growth of *mpk4–/–*[pXNGK4] promastigotes. Cell numbers of wild-type (◆), MPK4 transgenic *mpk4+/+*[pXNGK4] (●), and *mpk4–/–*[pXNGK4] null mutant clones 3 and 5 (○, solid and dashed lines, clone 3 and 5 respectively) were estimated by microscopic counting. The bars indicate standard deviations of a triplicate experiment.
D. Macrophage infection assay of *mpk4–/–*[pXNGK4]. Peritoneal macrophages were infected with control WT (◆), mpk4*+/+*[pXNGK4] (●) and *mpk4–/–*[pXNGK4] clone 3 (○) metacyclic-enriched parasite fractions and the numbers of intracellular parasites were estimated by nuclear staining and fluorescence microscopy. Two independent experiments with similar outcome were performed. The bars indicate standard deviations of a triplicate experiment.
E. *In vivo* analysis of the MPK4 null mutant. A total of 5×10^5 stationary-phase parasites of WT (◆), *mpk4+/+*[pXNGK4] (●), and *mpk4–/–*[pXNGK4] clone 3 and 5 (○, solid and dashed lines, clone 3 and 5 respectively) were inoculated into the hind footpad of female BALB/c mice and lesion formation was monitored by measuring the increase in footpad size. Groups of six mice were analysed for each parasite line and standard deviations of a triplicate experiment are indicated by bars.
F. FACS analysis. *mpk4+/+*[pXNGK4] and *mpk4–/–*[pXNGK4] parasites were recovered from infected footpads and GFP intensity of derived promastigotes of *mpk4+/+*[pXNGK4] (left panel) and facilitated null mutant *mpk4–/–*[pXNGK4] clone 3 (right panel) were monitored by FACS analysis before (dashed lines) and after passing through mice (solid lines). Untransfected parasites were included as background control (dotted line).

Finally, we extended the duration of negative selection to 15 passages to test for complete episome loss in the *mpk4+/+*[pXNGK4] control and its persistence in the null mutants. Following selection in either nourseothricin or GCV for 15 passages, parasites were plated on agar to obtain clonal populations, expanded in liquid culture in the absence of selection, and total protein extracts from five independent clones were analysed by Western blotting using anti-GFP antibody to test for the presence of the episome. No GFP was detected in *mpk4+/+*[pXNGK4] control parasites after GCV treatment suggesting complete episome loss (Fig. 2C). In contrast, GFP was detected in all *mpk4–/–*[pXNGK4] subclones after long-term negative selection at levels comparable to null mutants selected for the maintenance of pXNGK4 with nourseothricin. We ruled out that pXNGK4 persistence was due to spontaneous inactivation of the *HSV*-TK gene by mutation and thus abrogation of negative selection by direct sequence analysis, or by transfection of these cells with an additional MPK4 WT copy (pLEXSY-MPK4), which allowed efficient loss of pXNGK4 in the presence of GCV (data not shown and Fig. 4A). Together our results validate the pXNG vector as a powerful experimental system to genetically prove the essential nature of *Leishmania* genes as exemplified here for MPK4, which is critical for promastigote survival *in vitro*.

Negative selection by GCV is independent of cell death

We performed a series of control experiments to investigate in more detail the mechanism of negative selection. Compared to the two *mpk4–/–*[pXNGK4] clones selected with NTC, the same clones selected with GCV showed a transient reduction in cell growth during the first 3 days of the first passage in GCV medium (Fig. 3A, left panel), which was not due to cell death as shown by the absence of propidium iodide (PI) positive, dead cells (Fig. 3A, right panel). This indicates that GCV does not have a cytotoxic but a cytostatic effect on parasites causing a transient reduction in growth early during negative selection, which may be the consequence of a stress response. Increasing the GCV concentration by 10-fold did not result in any significant increase in parasite cell death, establishing GCV as a cytostatic rather than cytolethal drug in *Leishmania* (Fig. S1).

We routinely observed early during negative selection the emergence of a subset of *mpk4–/–*[pXNGK4] parasites that showed low fluorescence intensity similar to the WT control. In order to determine if this phenomenon reflects an unexpected loss of episome or simply results from reduced GFP expression in a fraction of parasites, the two populations GFP_{low} and GFP_{high} were separated by FACS sorting (Fig. 3B, left panel). After 24 h of culture in the absence of selective drugs, sorted GFP_{low} parasites largely recovered high levels of GFP intensity (Fig. 3B right panel), indicating that the decrease of GFP fluorescence intensity in the *mpk4–/–*[pXNGK4] GFP_{low} population is not due to episome loss but to a transient reduction in GFP expression, likely due to stress.

We next performed quantitative (q)PCR to validate the correlation between GFP fluorescence levels and episome copy number utilizing primer pairs specific for the nourseothricin resistance cassette (SAT_1, Table S2). Direct quantification of episome levels over five passages in GCV medium showed a more than 30-fold reduction in the *mpk4+/+*[pXNGK4] control but only a fourfold reduction in the *mpk4–/–*[pXNGK4] clone 3 (Fig. 3C). In conclusion, our results validate GFP levels as readout for episome copy

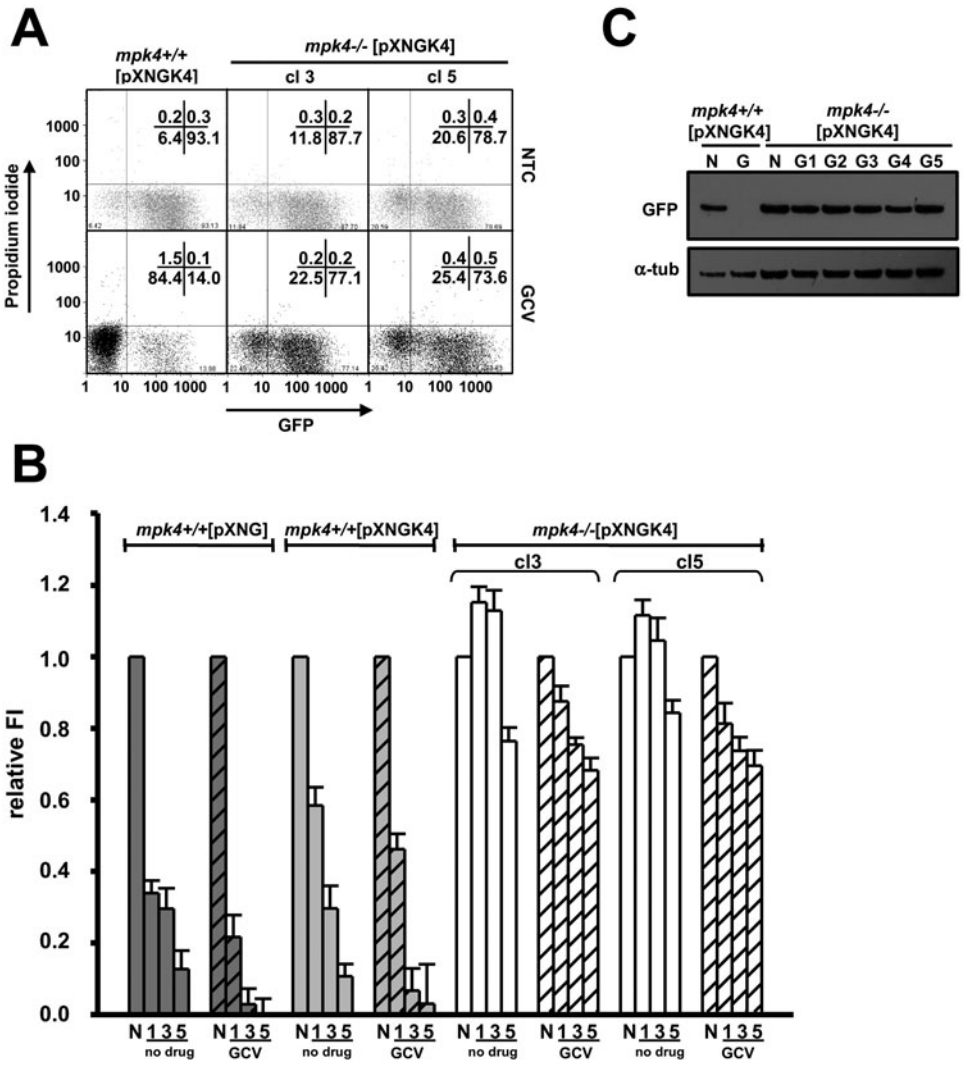

Fig. 2. *L. major* MPK4 is essential for *L. major* viability.
A. Analysis of *mpk4–/–*[pXNGK4] by negative selection. Presence of pXNGK4 was monitored by FACS analysis quantifying the expression levels of GFP encoded on the same plasmid. Control parasites *mpk4+/+*[pXNGK4] and facilitated null mutant *mpk4–/–*[pXNGK4] clones 3 and 5 cultured with 250 μg ml^{-1} nourseothricin (NTC, upper panel) or maintained for three culture passages with 50 μg ml^{-1} ganciclovir in the absence of nourseothricin (GCV, lower panel) are shown. Parasites were processed by flow cytometry and the number of GFP-positive cells (FL1-H, *x*-axis) and propidium iodide (PI)-positive dead cells (FL2-H, *y*-axis) were determined. The per cent of cells per quadrant is indicated by the numbers.
B. Time-course analysis. Promastigotes of *mpk4+/+*[pXNG], *mpk4+/+*[pXNGK4] and *mpk4–/–*[pXNGK4] null mutant clones were maintained for five culture passages without drug or in the presence of NTC (N) or GCV and were assessed for GFP expression levels by FACS analysis at each passage. The relative GFP mean fluorescence intensity (relative FI) was plotted for passages 1, 3 and 5. The bars indicate standard deviations of a representative triplicate experiment. Three independent triplicate experiments with similar outcome were performed.
C. Western blot analysis. *mpk4+/+*[pXNGK4] and *mpk4–/–*[pXNGK4] null mutant clone 3 were selected with either nourseothricin (N) or ganciclovir (G) for 15 culture passages, *mpk4–/–*[pXNGK4] null mutant clone 3 was spread on agar plates and five independent clones were selected (G1–G5). Total proteins were extracted from *mpk4+/+*[pXNGK4] pool or *mpk4–/–*[pXNGK4] clones and analysed by immunoblotting with anti-GFP antibody to reveal loss of pXNGK4, and anti-tubulin antibody for normalization.

number and demonstrate that negative selection by GCV does not result in a direct cytotoxic effect but is likely to cause cellular stress in parasites expressing *HSV*-TK from pXNG. Given identical results for *mpk4–/–*[pXNGK4] null mutant clones 3 and 5 all subsequent experiments were performed with only clone 3.

Structure–function analysis of LmaMPK4 by plasmid shuffle

Although LmaMPK4 is highly conserved and shows 42% sequence identity to human ERK2, multiple sequence alignment identified various sequence elements that

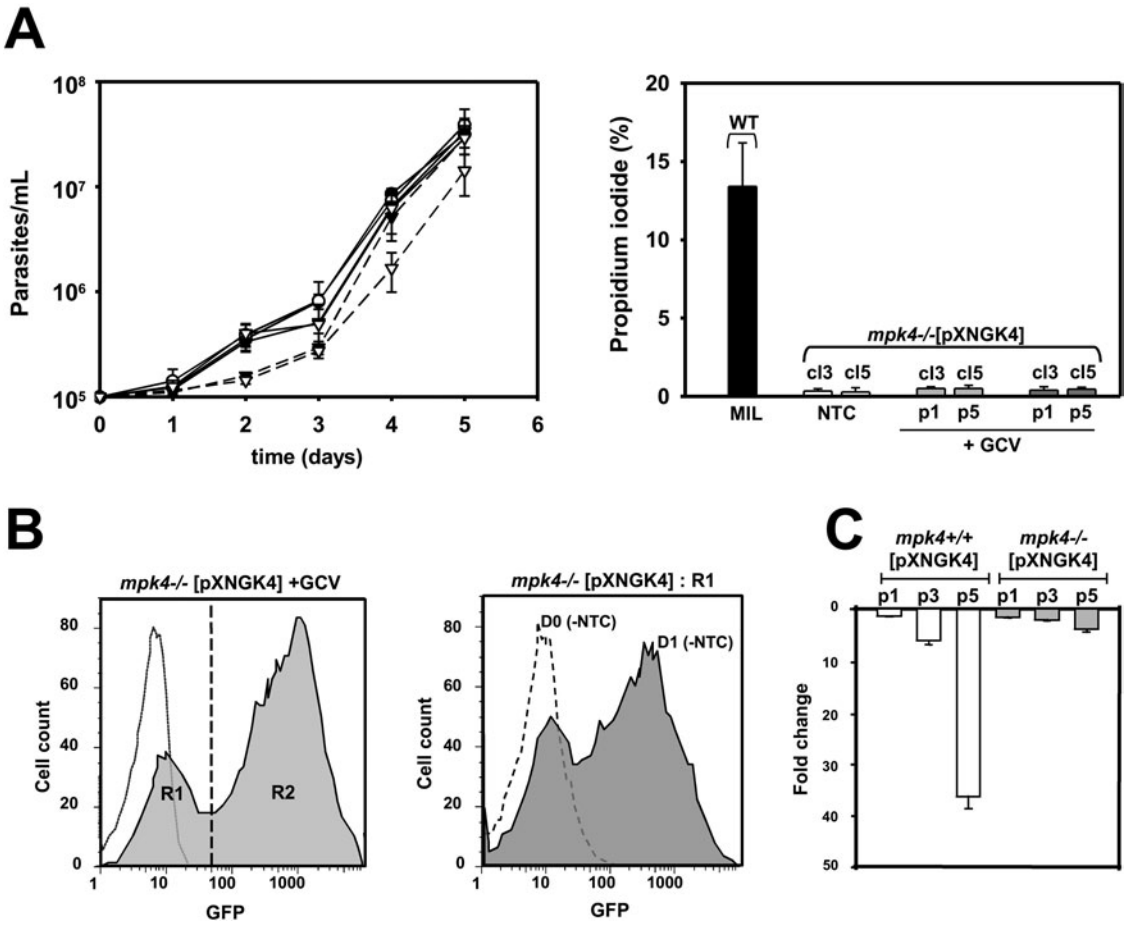

Fig. 3. Effect of ganciclovir treatment on *L. major* parasites.
A. Growth and cell death analyses of parasites treated with ganciclovir. Culture density (left panel) was estimated by microscopic cell counting for both *mpk4–/–*[pXNGK4] clones 3 and 5 maintained with nourseothricin (NTC) (● and ○ respectively) and cultured with GCV over 5 days during the first five passages (▼ and ▽ respectively). Results for passages (p) 1 and 5 in GCV (solid and dashed lines respectively) are shown. For cell death analysis, parasites were stained with propidium iodide and were assessed by FACS analysis (right panel). Miltefosine treated WT parasites (black bar) were used as positive control for parasite death. The bars indicate standard deviations of a triplicate experiment.
B. FACS sorting of *mpk4–/–*[pXNGK4] populations showing different levels of GFP fluorescence. Histogram plot representing the background fluorescence of untransfected control parasites (dotted line) and *mpk4–/–*[pXNGK4] parasite populations expressing GFP fluorescence at low (R1) and high levels (R2) (left panel). R1 and R2 populations were separated by FACS sorting and population R1 was placed in culture in the nourseothricin selection absence of drug. GFP fluorescence levels were investigated at day 0 (D0, dashed) and day 1 (D1, solid) by FACS analysis in the absence of nourseothricin selection (-NTC) (right panel).
C. Quantitative PCR. DNA was extracted from *mpk4+/+*[pXNGK4] (white bars) and *mpk4–/–*[pXNGK4] clone 3 (grey bars) promastigotes over the first five passages under GCV selection. qPCR was performed using primers specific for the resistance cassette against nourseothricin (SAT_1). Results for passage (p) 1, 3 and 5 in GCV are shown. The bars indicate standard deviations of a triplicate experiment.

may be exploited for drug development (Fig. S2A). Because of the essential nature of LmaMPK4 and the lethal null mutant phenotype, these sequence elements however escape functional analysis by classical genetic complementation. To overcome this limitation we further exploited our facilitated MPK4 null mutant system and performed a detailed structure/function analysis by applying a plasmid shuffle approach on various MPK4 derivatives structural and regulatory mutations, including (i) deletion of a highly parasite-specific N-terminal region (ΔN), (ii) mutation of the key lysine residue in ATP binding pocket (K59A) that is the prime target for pharmacological kinase inhibition, and (iii) mutation of the TQY motif [T190A, Y192F, Q191E and T190A-Y192F (T/A-Y/F) double mutant] required for kinase activation by upstream MKKs (Fig. S2A and B).

Control (WT) and mutated LmaMPK4 genes were inserted in vector pLEXSY-neo2 (Jena Bioscience) and transfected into *mpk4–/–*[pXNGK4] clone 3. Transfected pools were grown in medium supplemented with 250 μg

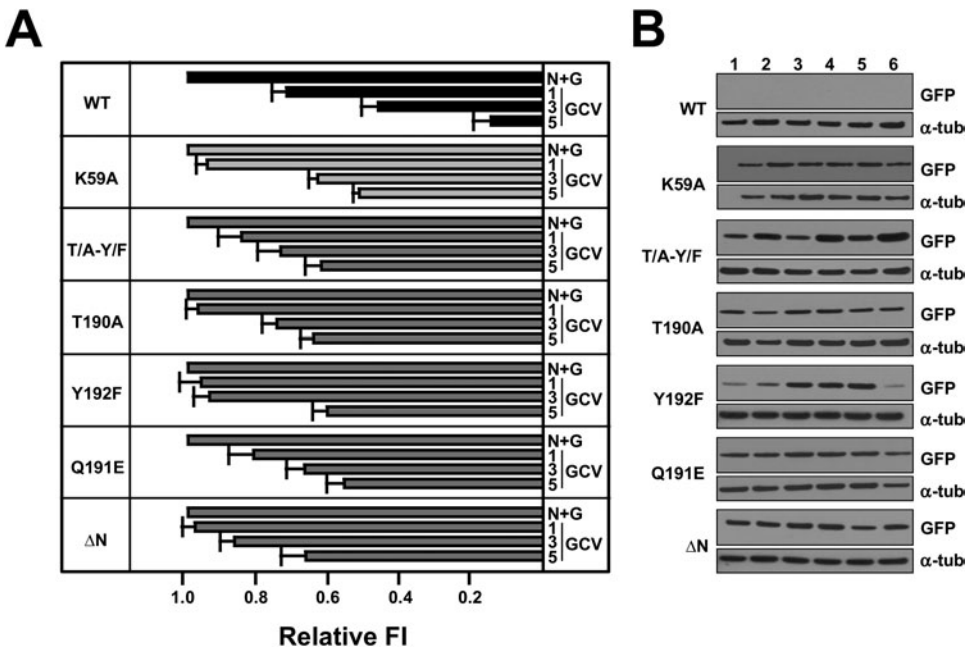

Fig. 4. *L. major* MPK4 structure/function analysis by plasmid shuffle.
A. Time-course analysis. *mpk4–/–*[pXNGK4] lines expressing pLEXSY-MPK4-WT (black bars) or the indicated MPK4 mutants (grey bars) either were maintained in 250 μg ml^{-1} nourseothricin (N) and 100 μg ml^{-1} geneticin (G) to select for both episomes (N+G) or were incubated for five passages with 50 μg ml^{-1} ganciclovir (GCV) for negative selection against pXNG-MPK4. Parasites were assessed for GFP expression levels by FACS analysis at passages 1, 3 and 5. The MPK4 mutation status of these lines is indicated at the left of the panel. The bars indicate standard deviations of a representative triplicate experiment. Two independent triplicate experiments with similar outcome were performed. FI, fluorescence intensity.
B. Western blot analysis. After 15 culture passages in the presence of GCV, six individual clones of *mpk4–/–*[pXNGK4] expressing the indicated MPK4 mutants from pLEXSY-neo2 were isolated (clones 1–6) from plates supplemented with GCV. Total proteins were extracted and analysed by immunoblotting with anti-GFP antibody to assess the presence or absence of pXNGK4, and with anti-tubulin antibody for normalization.

ml^{-1} nourseothricin and 100 μg ml^{-1} geneticin to select for both pXNG and pLEXSY plasmids. Plasmid shuffle, i.e. loss of the pXNGK4 episome in the presence of pLEXSY-driven expression of either MPK4 WT (positive control) or the various MPK4 mutants, was evaluated by FACS analysis during several passages in medium containing GCV only (Fig. 4A). *mpk4–/–*[pXNGK4] parasites overexpressing pLEXSYK4-WT, referred to as *mpk4–/–*[pXNGK4][pLEXSYK4-WT], showed a rapid decrease in relative FI over five passages in GCV and eliminated pXNGK4 due to the presence of the additional MPK4 WT copy expressed from pLEXSY, thus validating our plasmid shuffle approach (Fig. 4A). As expected, expression of the kinase dead K59A mutant or the T190A and Y192F single, and T190A-Y192F double mutant did not result in significant reduction of relative FI levels during 5 days of negative selection, suggesting that both phosphotransferase activity and MPK4 phosphorylation by upstream MKKs are essential for MPK4 function. Likewise, expression of the ΔN and the Q191E mutant forms of MPK4 did not allow for pXNG-MPK4 removal attributing for the first time essential function to these rather unusual MAPK sequence elements. We further confirmed these results by long-term selection during 15 culture passages in GCV (Fig. 4B). Six individual clones for each negative selection were isolated on agar plates supplemented with GCV and expanded in liquid, and total protein extracts were analysed by Western blotting using anti-GFP antibody to assess the presence of the pXNG episome. The absence of GFP signals in *mpk4–/–*[pXNGK4][pLEXSYK4-WT] and its persistence in the null mutants expressing pLEXSY-MPK4ΔN, pLEXSY-K59A, or the pLEXSY-MPK4 TQY mutants genetically defines these sequence elements as essential for LmaMPK4 activity and *L. major* viability in culture.

Establishment of an MPK4 null mutant expressing MPK4 with altered ATP binding pocket

The requirement of MPK4 expression to compensate for the lethal null mutant phenotype in *mpk4–/–* precluded us to gain insight into the biological role of this kinase by loss-of-function analysis. However, using the plasmid shuffle approach provided an opportunity to test if we could establish a null mutant that expresses an enzymatically attenuated version of MPK4 that may allow *in vitro* parasite

survival but may be compromised in biological functions that depend on full MPK4 activity. We aimed to establish such a mutant by targeting the ATP binding site. A series of MPK4 mutants surrounding the key lysine residue implicated in ATP binding and orientation were generated (Fig. S2B). In particular, replacing the key lysine residue with arginine (K59R) has been previously shown in other protein kinases to result in reduction of phosphotransferase activity (Robinson *et al*., 1996) and thus was expected to alter MPK4-ATP interaction. We first investigated this possibility by structural modelling of the MPK4 ATP binding site of WT and K59R. Introduction of this mutation alters conserved ATP/residue interactions and reduces the volume of the binding pocket volume as R59 is positioned differently compared to K59 and extends into the cleft of the active site (Fig. 5A). We first confirmed ATP binding of this mutant by performing an ATP binding chromatography with purified recombinant MPK4 WT and K59R mutant. Briefly, ATP agarose was incubated with the protein samples, and flow-through as well as protein bound to the matrix were analysed by SDS-PAGE and immunoblotting. Both MPK4 WT and K59R mutant showed binding to the ATP matrix, which was efficiently competed by pre-incubation of the proteins with free ATP (Fig. 5B).

We next tested if MPK4-K59R retains phosphotransferase activity by plasmid shuffle. The MPK4 mutants K59R, R60A and K59A-R60A (K/A-R/A) (Fig. S2B) were cloned into pLEXSY-neo2 (Jena Bioscience), transfected into *mpk4–/–*[pXNGK4], and plasmid shuffle by negative selection was performed as described above. FACS analysis of two independently generated pools of *mpk4–/–*[pXNGK4][pLEXSYK4-K59R] exposed to short-term negative selection (pool 1 and pool 2, Fig. 5C), and Western blot analysis of six independent shuffle clones of pool 1 and 2 isolated from plates after long-term negative selection (Fig. 5D) revealed efficient loss of pXNGK4 providing the genetic proof that this mutant retains a level of MPK4 kinase activity compatible with *in vitro* promastigote survival. Significantly, efficient shuffle occurred only under negative selection as passive loss of pXNG-MPK4 (even under positive selection for pLEXSY-MPK4 with G418) occurred in only three out of six clones (Fig. S3). Likewise, the R60A MPK4 mutant retains activity based on the shuffle kinetics and the absence of GFP signal after long-term negative selection (Fig. 5C and D). As expected, no shuffle occurred using the kinase dead pLEXSYK4-K59A-R60A double mutant. As judged by quantitative RT-PCR using primers specific for MPK4 sequence (MPK4_1, Table S2), both MPK4 WT and MPK4 K59R were expressed in the respective shuffle lines (Fig. 5E and Fig. S4). In the following we assessed the phenotypic consequences of altered MPK4 activity in the *mpk4–/–*[pLEXSYK4-K59R] mutant.

mpk4–/–[pLEXSYK4-K59R] parasites show increased metacyclic development

Under normal growth conditions at pH 7.4, *mpk4–/–*[pLEXSYK4-K59R] shuffle clones corresponded in growth kinetics and morphology to untransfected WT and *mpk4–/–*[pLEXSYK4-WT] controls (Fig. 6A, and data not shown). We next assessed parasite growth at elevated temperature and acidic pH to test if MPK4 may play a role in stress-induced parasite differentiation. Both WT and mutant failed to survive in culture at 34°C (data not shown). Surprisingly, challenging these parasites with acidic pH produced significant phenotypic differences: the *mpk4–/–*[pLEXSYK4-K59R] mutant grew faster than the *mpk4–/–*[pLEXSYK4-WT] control parasites and attained higher density during the first 3 days after inoculation (Fig. 6B). Furthermore, the *mpk4–/–*[pLEXSYK4-K59R] mutant maintained high density during 4 days at stationary growth phase, while both untransfected WT and the *mpk4–/–*[pLEXSYK4-WT] control showed a substantial reduction in parasite number after reaching stationary phase. These data suggest that expression of the MPK4-K59R mutant alters parasite pH-dependent signalling and/or increases resistance to acidic stress.

Acidic pH has been shown to trigger metacyclogenesis *in vitro* (Bates and Tetley, 1993). The pH-dependent growth phenotype observed in the *mpk4–/–*[pLEXSYK4-K59R] shuffle line primed us to investigate metacyclic differentiation in acidified stationary culture by PNA agglutination (Sacks *et al*., 1985). Surprisingly, we consistently observed a significant, fourfold increase in metacyclic-like parasites from the K59R shuffle line compared to the corresponding WT shuffle line, which was independent of culture pH and enrichment procedure as this difference was maintained under both neutral and acidic growth conditions (Fig. 6C) and metacyclic purification by Ficoll gradient centrifugation (Fig. 6D) (Spath and Beverley, 2001) respectively. To investigate this phenotype in more detail we performed a time-course analysis of metacyclic differentiation in both WT and K59R shuffle lines over 6 days of culture in acidic medium. Briefly, WT and K59R shuffle lines were seeded at 2×10^6 p ml^{-1} and PNA enrichment was performed daily. No significant difference was observed between both lines during the first 2 days of culture (Fig. 6E). At day 3 of culture (corresponding to day 2 at stationary phase), the percentage of PNA(–) parasites attained 4% in the WT shuffle line and was steadily increased up to 6% over the course of the experiment. The K59R shuffle line attained 20% of PNA(–) parasites at day 3, which was maintained at high levels until day 5 of culture and slightly reduced at day 6. Thus expression of MPK4-K59R enhances the development of metacyclic-like parasites in culture.

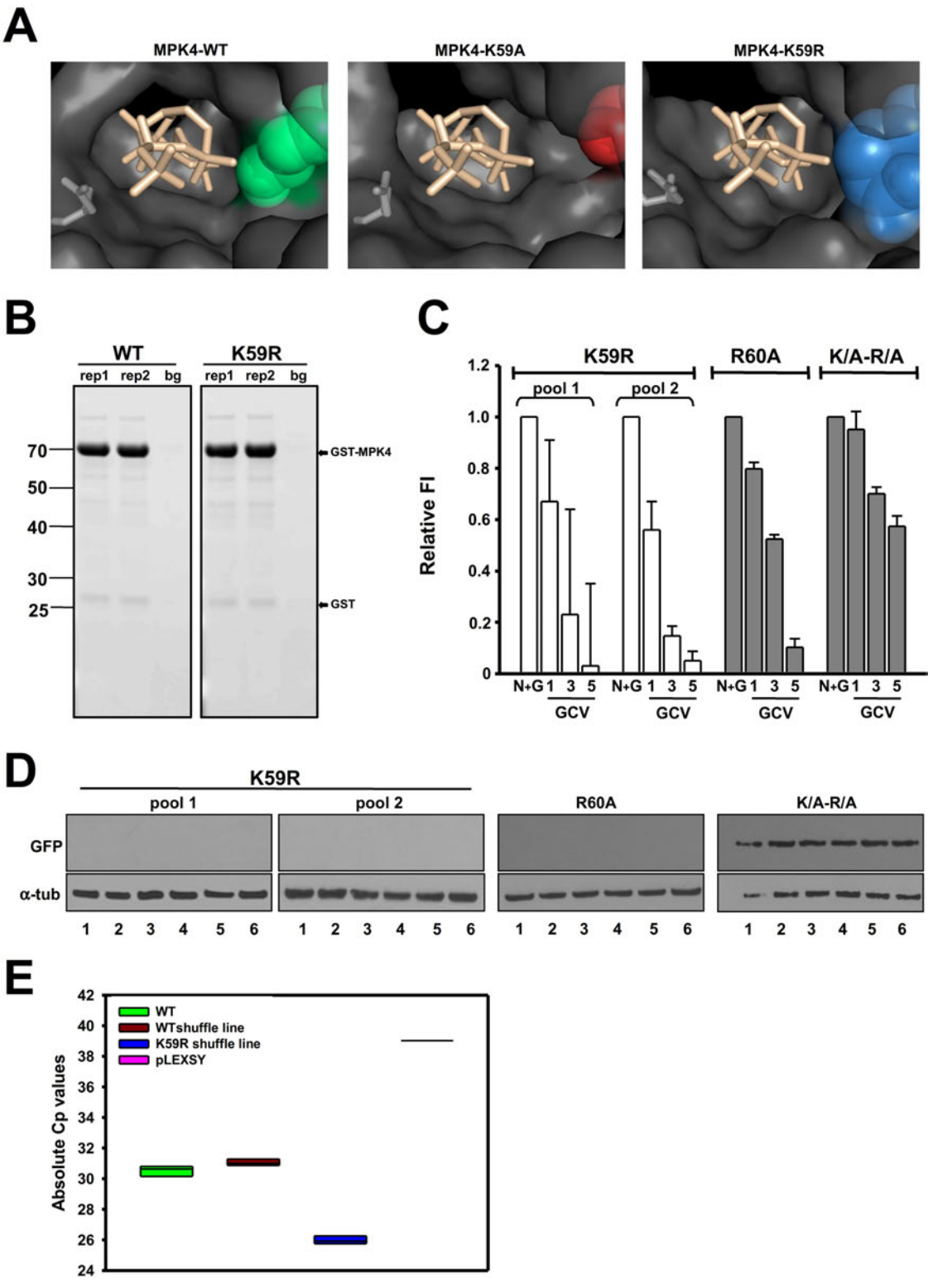

Fig. 5. Establishment of an MPK4 null mutant expressing MPK4 with altered ATP binding pocket.
A. Structural modelling. Comparison of the structural models of MPK4-WT (left panel) and the mutants K59A (middle panel) and K59R (right panel). ATP is represented in yellow.
B. ATP binding chromatography with recombinant MPK4. Purified GST-tagged MPK4-WT or K59R were incubated with 6AH-ATP-agarose (Jena Bioscience) in two replicates (rep 1 and 2), and recovered after boiling the ATP-agarose at 95°C for 10 min in the presence of sample loading buffer and reducing agent. The proteins were separated by SDS-PAGE and revealed by Western blotting. Empty agarose beads were used as control for binding specificity (background, bg). Molecular weight is indicated in kDa.
C. Time-course analysis of negative selection. *mpk4–/–*[pXNGK4] lines expressing MPK4 K59R (two independent parasite pools, white), R60A and K59R-R60A mutants from vector pLEXSY-neo2 either were maintained in nourseothricin (N) and geneticin (G) to select for both episomes (N+G) or were incubated for five passages with ganciclovir alone (GCV), and parasites were assessed for GFP expression levels by FACS analysis at each passage. The bars indicate standard deviations of a representative triplicate experiment. Three independent triplicate experiments with similar outcome were performed. FI, fluorescence intensity.
D. Western blot analysis. After 15 culture passages in the presence of GCV, six individual clones of *mpk4–/–*[pXNGK4] expressing the indicated MPK4 mutants from pLEXSY-neo2 were isolated (clones 1–6) from plates supplemented with GCV. Total proteins were extracted and analysed by immunoblotting with anti-GFP antibody to assess the presence or absence of pXNGK4, and with anti-tubulin antibody for normalization.
E. Detection of MPK4 transcripts in mutant lines by RT-qPCR. mRNA from untransfected WT control (green), *mpk4–/–*[pLEXSYK4-WT] (dark red) and *mpk4–/–*[pLEXSYK4-K59R] (blue) parasites was purified, retro-transcribed into cDNA, and the MPK4 transcripts were quantified by qPCR using specific primers (MD32/MD33, Table S2). The box plots illustrate the absolute Crossing point (Cp) values for three biological replicates performed in three technical replicates for each sample. Note that in this analysis the level of expression is inversely correlated with the Cp value (high Cp for the vector control).

mpk4–/–[pLEXSYK4-K59R] metacyclic parasites are attenuated in intracellular macrophage infection

We next tested the capacity of these metacyclic parasites to establish intracellular infection in peritoneal exudate macrophages (PEMs) obtained from BALB/c mice. PEMs were seeded on coverslips in 24-well plates and incubated with Ficoll enriched *mpk4–/–*[pLEXSYK4-K59R] and *mpk4–/–*[pLEXSYK4-WT] metacyclics at a multiplicity of five parasites per host cell. Non-ingested extracellular parasites were removed after 4 h of incubation by washing and intracellular parasite survival was monitored over 5 days by nuclear staining and fluorescence microscopy as described (Spath *et al*., 2000). Both lines established infection with similar efficiency showing 40% of infected macrophages hosting a mean of two parasites per host cell at the initial time point (Fig. 7A, upper panel). While the percentage of macrophages infected with the WT shuffle line remained constant over the entire infection period, suggesting efficient parasite survival, the infection levels of the K59R shuffle line dropped by more than twofold after 5 days (Fig. 7A, upper and middle panels), indicating clearance of a fraction K59R metacyclics by the host cell and thus attenuation of intracellular parasite survival. However, despite this clearance, the number of parasites per infected cells was similar between K59R and WT control during the 5-day infection experiment (Fig. 7A, lower panel). Thus, a fraction of *mpk4–/–*[pLEXSYK4-K59R] metacyclics seems normal in intracellular parasite survival, amastigote differentiation and proliferation. This observation is further sustained by PEM infection using stationary-phase parasites (Fig. 7B). In contrast to purified metacyclics, no difference in infectivity was observed with stationary-phase parasites despite the presence of fourfold more PNA(–) parasites in the K59R shuffle line. These profiles demonstrate that the increase in abundance of PNA(–) parasites in MPK4 K59R culture does not correlate with an increase in infectivity, suggesting a specific defect in a fraction of K59R cells and implicating LmaMPK4 phospho-transferase activity in the normal development of infectious *L. major* metacyclics. This possibility was further sustained by investigating metacyclic-specific cell size by FACS analysis using forward scatter (FSC) as read out. While metacyclic WT shuffle parasites produced a single narrow peak, two distinct populations were distinguished in K59R metacyclics, with one population showing WT profile, and a second one showing a significant increase in FSC and thus cell body size (Fig. 7C). In conclusion, expression of MPK4-K59R in the *mpk4–/–* null mutant results in the development of a fraction of metacyclic parasites that are altered in morphology and fail to establish intracellular infection despite a metacyclic-specific agglutination profile.

Discussion

The absence of robust and tightly controlled inducible expression systems in *Leishmania* precludes the study of essential genes by conditional null mutant analysis due to lethal knockout phenotypes. This limitation renders the biologically most significant genes inaccessible for loss-of-function studies and structure–function analyses by genetic complementation, with important negative impact on our understanding of *Leishmania*-specific biology and the identification and validation of novel drug targets. Here we exploit a negative selectable vector system applied on the *Leishmania* MAP kinase MPK4 to render loss-of-function analysis of essential *Leishmania* genes highly

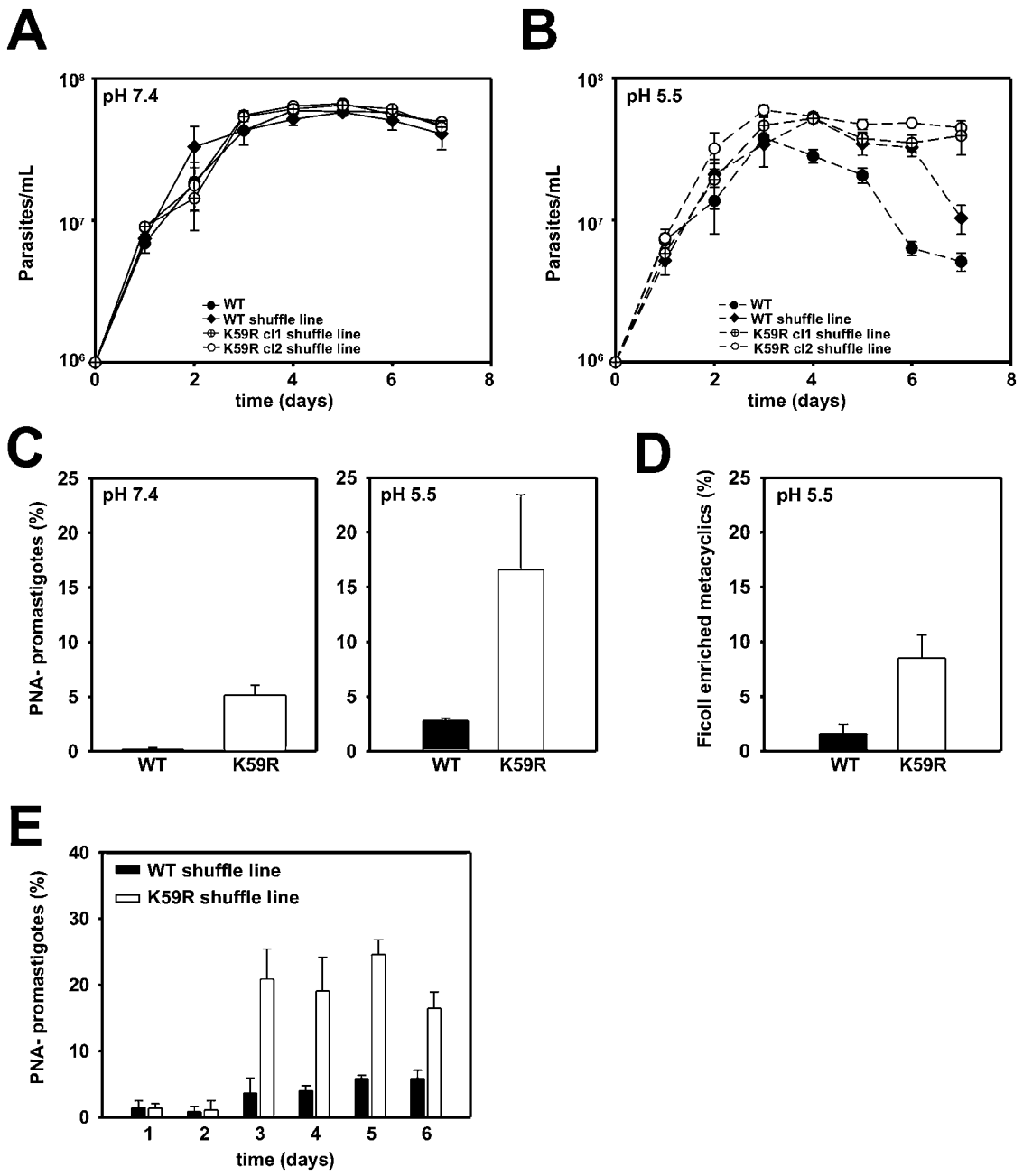

Fig. 6. *mpk4–/–*[pLEXSYK4-K59R] parasites show increased metacyclic development.
A and B. Culture density of WT control (●), *mpk4–/–*[pLEXSYK4-WT] (◆, WT shuffle line) and *mpk4–/–*[pLEXSYK4-K59R] clone 1 and 2 (⊕ and ○, respectively, K59R shuffle lines) cultured at either pH 7.4 (A) or pH 5.5 (B) was determined over 7 days by microscopic cell counting using a haemocytometer. The bars indicate standard deviations of a triplicate experiment.
C. Analysis of metacyclogenesis by PNA agglutination. *mpk4–/–*[pLEXSYK4-WT] and *mpk4–/–*[pLEXSYK4-K59R] parasites were suspended at 2×10^6 parasites ml^{-1} at pH 7.4 and pH 5.5 (left and right panels respectively) and metacyclic-like parasites were isolated by PNA agglutination at day 3 corresponding to day 2 stationary phase. The percentage of non-agglutinated *mpk4–/–*[pLEXSYK4-WT] (black bars, WT) and *mpk4–/–*[pLEXSYK4-K59R] (white bars, K59R) metacyclic parasites is represented. The bars indicate standard deviations of a representative duplicate experiment. Three independent duplicate experiments with similar outcome were performed.
D. Enrichment of metacyclic parasites by Ficoll gradient centrifugation. *mpk4–/–*[pLEXSYK4-WT] and *mpk4–/–*[pLEXSYK4-K59R] parasites were suspended at 2×10^6 parasites ml^{-1} at pH 5.5 and metacyclic-like parasite were isolated by density centrifugation using a Ficoll gradient. The percentage of Ficoll enriched metacyclics is represented. The bars indicate standard deviations of a representative duplicate experiment. Two independent duplicate experiments with similar outcome were performed.
E. Time-course analysis of metacyclogenesis. The number of PNA(–) metacyclic parasites of *mpk4–/–*[pLEXSYK4-WT] (black bars, WT) and *mpk4–/–*[pLEXSYK4-K59R] (white bars, K59R) shuffle lines cultured at pH 5.5 was determined over 6 days by microscopic cell counting using a haemocytometer. The bars indicate standard deviations of a triplicate experiment.

informative, and to exploit the lethal null mutant phenotype to probe for druggability potential and gene function.

A first challenge in the analysis of essential *Leishmania* genes is represented by establishing a definitive proof of their requirement for parasite viability. Unlike in *Trypanosoma brucei*, where essential gene function can be directly investigated through conditional siRNA knock-down or knockout approaches (Ngo *et al*., 1998; Bastin *et al*., 2000; Shi *et al*., 2000), the proof of essentiality for a given gene in *Leishmania* is established indirectly by the failure to generate homozygous null mutants and their rescue by introduction of an episomal copy of the target gene. This approach has been applied for the study of many parasite genes encoding for structural, biosynthetic, or signalling proteins (Mottram *et al*., 1996; Hassan *et al*., 2001; Agron *et al*., 2005; Vergnes *et al*., 2005; Wang *et al*., 2005; Mukherjee *et al*., 2009; Wiese *et al*., 2009). For example, null mutants of the *L. mexicana* MAP kinase homologue MPK4 could only be established in transgenic parasites expressing an episomal copy of MPK4, which was maintained in culture and during *in vivo* infection even in the absence of selection, suggesting its requirement for both stages (Wang *et al*., 2005). However, neither result provides a direct proof for essentiality as the presence and persistence of episomal MPK4 may just reflect a selective advantage in growth or survival rather than essential gene function. To distinguish between these possibilities and establish the definitive genetic proof of MPK4 essentiality, we generated a facilitated *L. major* MPK4 null mutant using the pXNG vector system that was initially described by Murta *et al*. (2009) and allows for efficient negative selection against the episome due to the presence of the *Herpes simplex* virus thymidine kinase gene that renders transgenic parasites susceptible to the anti-viral drug ganciclovir (Muyombwe *et al*., 1997; Ghedin *et al*., 1998; Murta *et al*., 2009; Morales *et al*., 2010b; Feng *et al*., 2013). Treatment of the pXNG-MPK4 transgenic wild-type control *in vitro* with GCV caused a strong negative selection as documented by the complete elimination of pXNG-MPK4 over 15 passages. In contrast, the pXNG-MPK4 persisted in MPK4 null mutant clones despite considerable stress caused by negative selection, which was not due to inactivation of the negative selection marker *HSV*-TK by mutation as shown by sequence analysis. These results thus establish the definitive genetic proof that MPK4 is indispensable for promastigotes in culture and demonstrate the power of the pXNG vector system to distinguish between genes that may simply provide a selective growth advantage from those with non-redundant and essential function.

A second important limitation for the analysis of essential genes is represented by the failure to assess structure/function relationships by genetic complementation. In viable null mutants, sequence elements can be easily probed for their function by mutagenesis and testing the capacity of the mutant versions to restore wild-type phenotype upon expression in knockout cells. The requirement of an extra copy of the wild-type target gene in lethal null mutants precludes this analysis, which is especially frustrating for protein families with good druggability potential. One family that has attracted considerable interest in parasite drug target discovery is represented by protein kinases (Naula *et al*., 2005): they (i) are linked to environmentally induced, adaptive stage differentiation essential for host infection in *Plasmodium* (Rangarajan *et al*., 2005; Dorin-Semblat *et al*., 2007), *T. brucei* (Muller *et al*., 2002; Domenicali Pfister *et al*., 2006; Bao *et al*., 2010), and *Leishmania* (Wiese, 1998; Morales *et al*., 2007), (ii) are structurally divergent from mammalian protein kinases (Saravanan *et al*., 2010; Ojo *et al*., 2011; Horjales *et al*., 2012), and (iii) benefit from the interest of pharmaceutical companies to develop new anti-kinase drugs thus providing access to dedicated combinatorial compound libraries and high-throughput capable screening assays. Recent publications exploiting an MPK4 structural model identified this kinase as a potential target for anti-leishmanial alkaloid compounds by virtual screening (Ghosh *et al*., 1985; Gupta *et al*., 2013), and discussed the druggability potential of various MPK4-specific features, including an N-terminal extension or the presence of an unusual TQY motif in the activation loop (Saravanan *et al*., 2010). We applied the pXNG system to test for the requirement of these sequence elements for MPK4 function using a plasmid shuffle approach, which tests for the capacity of a second episome expressing a mutant version of the kinase to replace the pXNG-MPK4 wild-type copy during negative selection. Based on the failure of MPK4 mutant derivatives to replace pXNG-MPK4 we could attribute essential function to (i) the N-terminal domain, which may be required for protein localization, stabilization, or regulation as proposed for mammalian ERK1 (Roskoski, 2012) and ERK5 (Yan *et al*., 2001), (ii) the highly conserved lysine residue at position K59 implicated in ATP-orientation and essential for protein kinase activity (Carrera *et al*., 1993), thus demonstrating that MPK4 is not a pseudo-kinase but that its function is dependent on phosphotransferase activity, (iii) the regulatory T and Y residues in the activation loop, which are dually phosphorylated by upstream MAPK kinases, thus confirming the presence of a MPK4-specific MAPK cascade likely implicating MKK5 (John von Freyend *et al*., 2010), and (iv) the unusual central glutamine residue of the TXY motif, which most commonly is occupied by glutamate or aspartate, and is shared with only few other MAP kinases, including *Leishmania* MPK12 (Wiese, 2007), and two stress kinases in *Caenorhabditis elegans* and *Aedes aegypti* (Wiese, 2007). Together these data allow important new insight into MPK4 regulatory sequence elements and significantly increase the druggability potential of this kinase, which

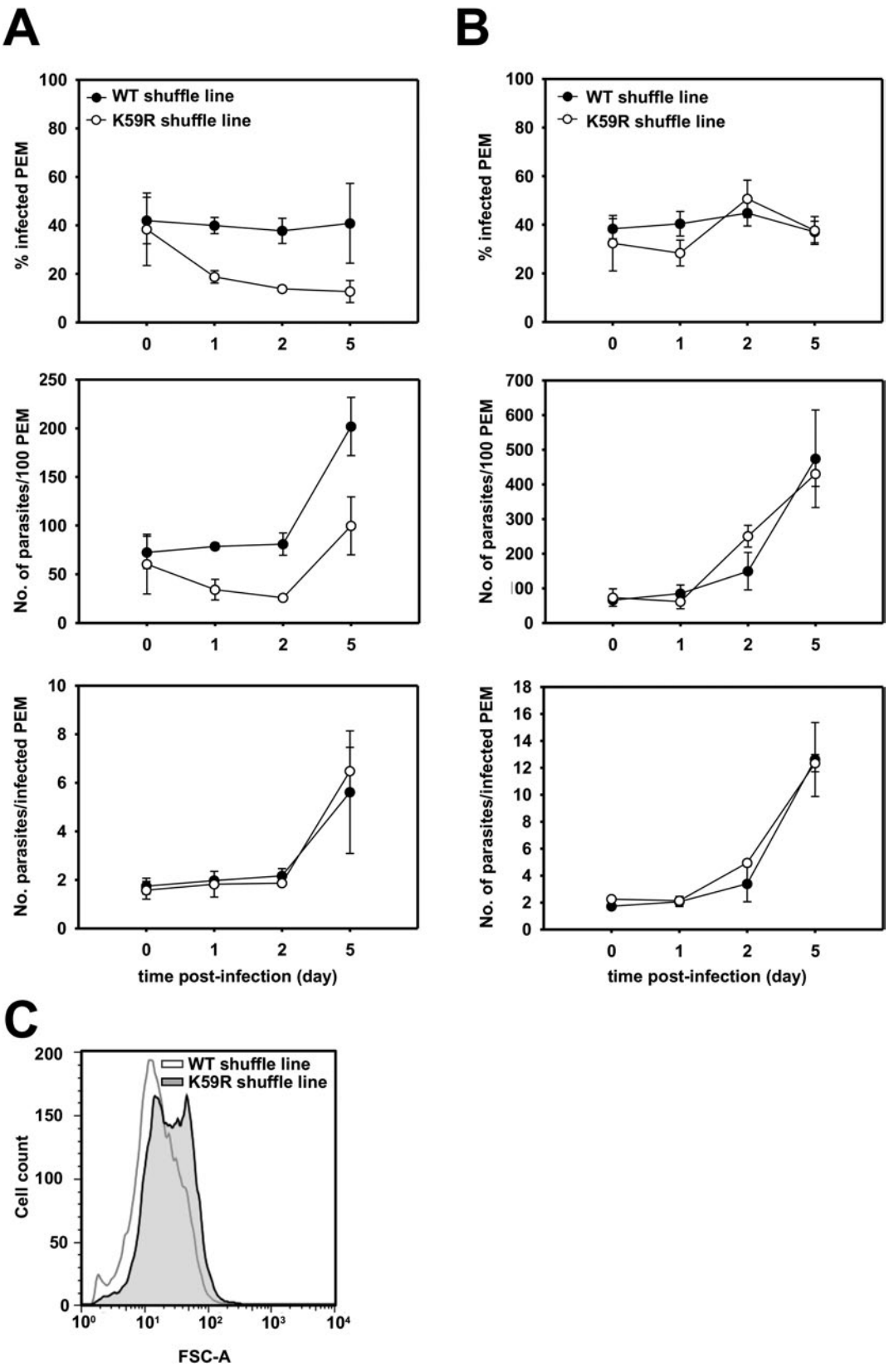

Fig. 7. *mpk4–/–*[pLEXSYK4-K59R] parasites show reduced intracellular macrophage survival.
A and B. PEM infection with metacyclic-enriched (A) and stationary (B) parasites. BALB/c peritoneal exudate macrophage (PEM) were infected for 4 h at 34°C with *mpk4–/–*[pLEXSYK4-WT] (●, WT shuffle line) and *mpk4–/–*[pLEXSYK4-K59R] (○, K59R shuffle line) metacyclic parasites enriched by Ficoll gradient centrifugation at a multiplicity of five parasites per host cell (A), and stationary-phase parasites at a multiplicity of 10 parasites per host cell (B). Percentage of infected macrophages (upper panels), number of intracellular parasites per 100 PEM (middle panels) and number of parasites per infected cells (lower panels) were determined at day 0, 1, 2 and 5 post infection by nuclear staining with Hoechst 33341 and fluorescence microscopy. The bars indicate standard deviations of a representative triplicate experiment. Three independent duplicate experiments with similar outcome were performed.
C. Cell size analysis. The size of *mpk4–/–*[pLEXSYK4-WT] (open histogram) and *mpk4–/–*[pLEXSYK4-K59R] (grey histogram) metacyclics were analysed by FACS using forward scatter (FSC) as read out.

could be efficiently inhibited by either classical competitive drugs targeting the ATP binding site, or allosteric inhibitors affecting kinase conformation and productive ATP binding by interaction with the parasite-specific N-terminal domain or the unusual activation loop.

Finally, the most important bottleneck in the study of essential *Leishmania* genes is the lethal null mutant phenotype itself, which strongly limits our insight into the function of the biologically most relevant genes. By utilizing a structure-informed genetic approach to generate a MPK4 mutant with altered ATP-binding properties we provide here a first proof-of-principle that negative selection combined with plasmid shuffle can establish a partial mutant with discernible phenotypic defects. Despite all our efforts, direct assessment of MPK4 kinase activity of this mutant failed using bacterially expressed, GST-tagged MPK4 alone or coexpressed with its putative activating kinase MKK5 (John von Freyend *et al*., 2010) (Fig. S5A). Likewise, GFP-tagged MPK4 obtained from transgenic parasites failed to yield robust and specific signals towards generic kinase substrates (Fig. S5B), even though the tagged kinase is fully active as judged by efficient plasmid shuffle of pXNG-MPK4 (Fig. S5C). These data suggest that MPK4 activity may be highly substrate-specific or dependent on interactions that are lost during protein purification. However, our plasmid shuffle analysis genetically validated that the K59R mutant retains activity. The high conservation of the MPK4 ATP binding site to ERK2, for which reduced phosphotransferase activity of the corresponding K to R mutant has been experimentally validated (Posada and Cooper, 1992; Robbins *et al*., 1993), strongly supports attenuation of MPK4-K59R phosphotransferase activity. Analysis of this K59R shuffle line established a link between MPK4 and both gain and loss of biological functions. First, we routinely observed that the K59R shuffle line showed more robust growth in acidic medium compared to control, suggesting either a gain in pH tolerance or a loss in pH sensing. Second, the K59R shuffle line showed a fourfold increase in the number of PNA(–), metacyclic-like parasites during stationary growth phase, which however were compromised in intracellular survival, indicating a gain in environmentally induced metacyclic development but a loss of virulence function. Together these data are compatible with the hypothesis that MPK4 is a stress kinase likely implicated in pH sensing required for proper metacyclic differentiation and parasite infectivity. Similar to ERK2, MPK4 is likely attenuated in kinase activity and thus the phenotypic effects may result from under-phosphorylation of MPK4-specific substrates. A role of MPK4 in virulence and stress signalling is further supported by the respective observations that pXNG-MPK4 is amplified in MPK4 facilitated null mutants during mouse infection, and that the central glutamine residue of the TXY motif carries essential function, thus classifying MPK4 as a member of the stress-activated protein kinase (SAPK) family (Kultz, 1998).

In conclusion, by applying a series of novel approaches based on the negative selectable episome pXNG we could overcome important limitations imposed on loss-of-function study of essential genes, and exploit the lethal null mutant phenotype to gain insight into kinase regulation, function and druggability. Several important questions remain to be addressed. Even though MPK4 is essential for promastigote viability and beneficial for amastigote infectivity *in vivo* as documented here for *L. major* and in a previous study for *L. mexicana* (Wang *et al*., 2005), the low yield of inactive recombinant protein and the failure to detect specific MPK4 activity in purified transgenic protein using various canonical substrates pose important limitations for a drug screening effort. Thus, a better understanding of the MPK4 activation mechanisms, the role of scaffolding proteins and molecular chaperones in regulating its phosphotransferase activity, and of MPK4 endogenous substrates will be crucial to assess the true potential of MPK4 as a valid drug target. Significantly, the approaches presented here are broadly applicable to any essential *Leishmania* gene and thus will have a major impact on our understanding of the biologically most relevant parasite genes and the discovery and validation of novel targets for anti-leishmanial chemotherapy.

Experimental procedures

Parasites

Leishmania major strain Friedlin V1 (MHOM/JL/80/Friedlin) was grown in M199 medium at 26°C (Kapler *et al*., 1990). Transgenic parasites were cultured in M199 medium supplemented with (i) hygromycin (30 μg ml^{-1}; Invitrogen) and puro-

mycin dihydrochoride (30 μg ml^{-1}; Sigma) to select for homologous recombination events, (ii) nourseothricin (NTC) (250 μg ml^{-1}; Jena Bioscience) and ganciclovir (GCV) (50 μg ml^{-1}; Invivogen) to respectively select for or against the episomal vector pXNG (Murta *et al*., 2009), kindly provided by S.M. Beverley), and (iii) G418 (100 μg ml^{-1}; Invitrogen) for selection of pLEXSY-neo2 (EGE-233; Jena Bioscience).

Generation of null mutant parasites

PCR-amplified sequences were verified by DNA sequencing (GATC Biotech). Primers used in this study are summarized in Table S1.

Generation of episomal construct pXNG-MPK4. A previously modified version of vector pXNG has been used with the original BglII site replaced by XhoI and AflII to facilitate cloning (primers MD1/MD2, Table S1) (Morales *et al*., 2010b). The endogenous gene of the putative *L. major* MAPK homologue LmjF.19.1440 (CAJ07240.1), designated as LmaMPK4, was amplified by polymerase chain reaction (PCR) from 100 ng genomic DNA of *L. major* FVI and was cloned into the pXNG XhoI site using primers MD3/MD4 (see Table S1) resulting in plasmid pXNGK4.

Generation of targeting constructs. The LmaMPK4 coding sequence was replaced with hygromycin (HYG) and puromycin (PAC) targeting cassettes by homologous recombination (LeBowitz, 1994). Approximatively 900 bp of LmaMPK4 5′UTR and 3′UTR were PCR-amplified and respectively cloned into pGEM-T® and pGEM-T® Easy vectors (Promega), resulting in pGEM-5′UTR and pGEM-3′UTR. The 5′UTR and 3′UTR for the HYG targeting construct were amplified using primers MD9/MD10 including PmeI/XhoI sites and primers MD11/MD12 including XmaI/PmeI sites (Table S1). For the PAC targeting construct, primers MD9/MD10 and primers MD11/MD13 with BglII/PmeI sites were used (Table S1). The 3′UTR insert was then released by NotI digestion and ligated into pGEM-5′UTR, resulting in construct pGEM-5′-3′UTR. The hygromycin and puromycin-resistance genes were obtained from pX63-HYG and pX63-PAC by digestion with XhoI/XmaI and XhoI/BglII, respectively, and were ligated directionally into pGEM-5′-3′UTR digested with the respective enzymes. The LmaMPK4 HYG and PAC targeting constructs were excised from the plasmid by PmeI digestion, dephosphorylated with Antarctic Phosphatase (NEB) and gel-purified. A total of 5×10^7 *L. major* promastigotes from logarithmic phase culture (density $< 5 \times 10^6$ ml^{-1}) were sequentially transfected with 20 μg of pXNG-MPK4 episome, then with 10 μg of the HYG targeting construct and finally with 10 μg of the PAC targeting construct, to establish the facilitated homozygous null mutant LmaMPK4 referred to in the following as *mpk4–/–*[pXNGK4]. Cells transfected with pXNGK4 were selected in liquid containing 150 μg ml^{-1} of NTC and were expanded in culture at drug concentrations up to 250 μg ml^{-1} of NTC. For the integration of HYG and PAC resistance cassettes, individual colonies after electroporation were isolated from M199 medium-1% agar plates (Noble Agar, Sigma) containing 60 μg ml^{-1} hygromycin or puromycin and 250 μg ml^{-1} NTC, and were expanded in liquid culture. Two independents clones of *mpk4–/–*[pXNGK4] were isolated and used for experiments. Parasites transfected with the pXNG vector alone were used as mock to control for non-specific effects associated with the plasmid, and WT parasites expressing pXNGK4 were used as positive control.

Confirmation of the mpk4–/–[pXNGK4] null mutant by PCR. The correct insertion of targeting constructs into the LmaMPK4 locus was verified by diagnostic PCR amplification. Primers p1/p2 and p1/p3 were used respectively to amplify the HYG and PAC recombinant cassettes in the genomic context (see Fig. 1A and Table S1). Primers p4/p5 were used to test for the presence of the LmaMPK4 ORF, while primers p6/p7 were used to amplify the cloned LmaMPK4 ORF from pXNG (Fig. 1A and Table S1).

Negative selection. For the negative selection against pXNGK4, the parasite medium containing 250 μg ml^{-1} NTC was replaced with medium containing 50 μg ml^{-1} GCV. Parasites were monitored for 15 passages by FACS analysis determining the levels of GFP expressed from the pXNG-MPK4 episome. Cell death was monitored simultaneously by propidium iodide staining. The loss of the pXNGK4 episome as determined by reduction in GFP fluorescence levels was evaluated after one, three and five passages in GCV by FACS. An end-point assessment after the 15 passages was performed by Western blot analysis. Briefly, *mpk4–/–*[pXNGK4] parasites were plated in the presence of 50 μg ml^{-1} GCV and six independent clones were isolated. Parasite proteins were extracted and 12 μg were analysed by SDS-PAGE and the presence or absence of the episome was revealed after blotting using an anti-GFP antibody (see below).

Plasmid shuffle analysis

Mutagenesis. All point mutations introduced in this study were generated by site-directed mutagenesis using the QuikChange® II XL Site-Directed Mutagenesis kit (Stratagene). The following mutations were performed in LmaMPK4: K59A, K59R, R60A, K59A-R60A, T190A, Y192F, T190A-Y192F, Q191E. The first 17 N-terminal amino acids of MPK4 were deleted to generate MPK4 mutant ΔN-ter. Corresponding primers are listed in Table S1 (from MD14 to MD29). Mutated sequences were verified by DNA sequencing (GATC Biotech).

L. major *pLEXSYK4 transfection.* Transgenic *L. major mpk4–/–*[pXNGK4] lines expressing WT or various mutated versions of LmaMPK4 were generated using vector pLEXSY-neo. The pLEXSY-MPK4 construct, designated as pLEXSYK4, was generated by inserting the 1.2 kb NcoI/KpnI fragment from pGEM-LmaMPK4 into the respective site of pLEXSY-neo (primers MD5/MD6, Table S1). The pLEXSY-ΔN-ter LmaMPK4 mutant was generated using primers MD7/MD6 (Table S1). *mpk4–/–*[pXNGK4] parasites were electroporated with the generated pLEXSYK4 constructs (see above). The LmaMPK4 null mutants carrying both pXNGK4 and pLEXSYK4, referred as *mpk4–/–*[pXNGK4][pLEXSYK4], were first maintained in 250 μg ml^{-1} NTC and 100 μg ml^{-1} G418 to obtain stable line.

Negative selection. The *mpk4–/–*[pXNGK4][pLEXSYK4] lines were cultured in medium containing 50 μg ml^{-1} GCV and

negative selection was performed as described above. Negatively selected parasites were assessed for GFP expression levels by FACS and Western blot analyses (see above).

PCR analyses

The LongAmp *Taq* PCR Kit (New England Biolabs) was used for gene cloning procedures. The PCR-mix consisted of 0.2 μM of forward and reverse primers, 1× reaction buffer with 1.5 mM of $MgCl_2$, 25 μM of each dNTPs, 10 ng of DNA and 1.25 units of polymerase in a total volume of 50 μl. The PCR-mix was initially denatured at 95°C for 5 min in a thermocycler (Bio-Rad) followed by 34 consecutive cycles of denaturing at 95°C for 30 s, annealing at 45–55°C for 30 s and extension at 65°C for 1–3 min (depending on the size of the amplification). A last extension step was carried out at 65°C for 10 min and samples were kept at 4°C until used.

Quantitative PCR. Primers used in these qPCR studies are summarized in Table S2. PCR were carried out in a 10 μl reaction volume on white opaque polypropylene wells (LightCycler® 480 Multiwell Plates 384) and were performed on a LightCycler® 480 system (Roche). Briefly, 2 μl of sample cDNA or DNA was added to 9 μl of a master mix containing 5 μl of QuantiFast SYBR Green Kit (Qiagen) and 4 μl of nuclease-free water with primers MD30/MD31 or MD32/MD33 (Table S2) (Sigma-Aldrich) at a final concentration of 0.5 μM. Activation of the Qiagen *Thermophilus aquaticus* polymerase was performed at 95°C for 5 min. The PCR programme included 45 cycles of denaturation at 95°C for 30 s, annealing coupled with extension at 60°C for 30 s. SYBR Green fluorescent emission was measured at the end of the elongation step. Subsequently, a melting curve programme was applied with a continuous fluorescent measurement starting at 60°C and ending at 95°C (ramping rate of 0.1°C s^{-1}).

PCR data statistical analyses. Relative quantitative data analysis, based on the method of Pfaffl (Pfaffl, 2001), was adapted from Prina *et al*. (2007). Briefly, the relative quantities of plasmid DNA target in different samples were computed based on the amplification efficiency and Cp deviation between tested sample and control. Cp values for the host ssrRNA reference gene (EP1/EP2, Table S2) were used for data normalization.

Multiple sequence alignment

Leishmania spp. and *Trypanosoma* spp. gene and protein sequences were retrieved from the web databases GeneDB (http://www.genedb.org) (Hertz-Fowler *et al*., 2004) and TriTrypDB (http://tritrypdb.org/tritrypdb/) (Aslett *et al*., 2010). The gene and protein sequences of other eukaryotes, i.e. human and yeast, were retrieved from either the databases NCBI Protein (http://www.ncbi.nlm.nih.gov/protein/) or Uniprot (Apweiler *et al*., 2004) (http://www.uniprot.org/). Homology searches were carried out using BLAST Programs with the default BLOSUM-62 substitution matrix. Multiple sequence alignment of MPK4 homologues was performed using built-in algorithm ClustalXv2. Additional sequence analysis was carried out using programs in the BioEdit Program suite (Tom Hall, North Carolina State University).

3D modelling

Structures of the ATP binding site of WT and mutant *L. major* LmaMPK4 interacting with ATP shown in Fig. 5A were built using the software MODELLER9v12 (http://salilab.org/modeller/) based on satisfaction of spatial restraints. Quality of the 3D structure homology models with ATP were ranked by Discrete Optimized Protein Energy (DOPE) score and the best model with the lowest DOPE score is shown. The 3D modelling was adapted from Saravanan *et al*. (2010).

Expression and purification of GST-LmaMPK4 in Escherichia coli

An N-terminal Glutathione *S*-Transferase (GST)-LmaMPK4 fusion construct was generated in plasmid pGEX-5X-1 (GE Healthcare). The 1.2 kb EcoRV–XhoI fragment from pGEM-LmaMPK4, referred to as pGEXK4, was inserted into the respective site of pGEX-5X-1 (primers MD8/MD4, Table S1). For the production of recombinant protein, bacterial strain Rosetta 2 (DE3) (VWR) was transformed with 2 μl of pGEXK4 and 50 ml of pre-culture was prepared. Twenty millilitres from this culture was used to inoculate 1 l of LB broth and incubated at 37°C on a shaker until cell density reached an OD of 0.6, then fusion protein expression was induced by 0.2 mM IPTG and the culture was further incubated overnight. The recombinant protein purification was adapted from Schmidt-Arras *et al*. (2011).

ATP binding assay

ATP binding was assessed using the ATP affinity Test Kit (AK-102, Jena Bioscience). All binding, washing and elution buffers were prepared according to the kit's manual. Twenty-five micrograms of recombinant GST-tagged MPK4 proteins were dialysed overnight and were applied to 25 μl of 6AH-ATP-agarose matrix to test for binding. Briefly, the agarose-sample mixtures were incubated on a roller for 2 h 30 at 4°C and were then eluted for 1 h at 4°C. The flow-through and elution fractions were collected, and the agarose matrix was mixed with 2× loading buffer and 8× reducing agent, boiled at 95°C for 10 min and proteins were collected. The obtained flow-through, elution fraction and matrix were analysed by SDS-PAGE and immunoblotting.

Protein extraction and Western blot analysis

A total of 10^9 cells from logarythmic growth phase of *L. major* promastigote cultures (density $< 5 \times 10^6$ ml^{-1}) were pelleted by centrifugation for 10 min at 4°C and 1500 *g*. Supernatants were removed, and cells were washed once in M199 medium for promastigotes. Cell pellets were resuspended in 1 ml lysis buffer containing 150 mM NaCl, 1% Triton X-100, 50 mM Tris-HCl and protease inhibitor cocktail (Roche). Samples were incubated for 30 min at 4°C and vortexed every 10 min. Following the removal of cellular debris by centrifugation, total protein extracts were quantified by using the Coomassie (Bradford) protein assay kit (Pierce). Total protein extracts were separated on 4–12% Bis-Tris NuPAGE® gels (Invitrogen) and blotted onto polyvinylidene difluoride (PVDF) membranes

(Pierce). Proteins were revealed using the following antibodies at the indicated dilutions: monoclonal anti-GFP horseradish peroxidase (HRP)-conjugated antibody (Miltenyi Biotec), 1:5000; mouse monoclonal anti-α-tubulin antibody (Sigma), 1:20 000; and anti-mouse HRP-conjugated secondary antibody (Invitrogen) 1:20 000. Blots were developed using SuperSignal Chemiluminescent detection system (Pierce) and visualized on X-ray film at various exposure times.

Growth determination

Parasite cell numbers were determined microscopically by counting 2% (w/v) glutaraldehyde fixed cells loaded in a Neubauer-improved cell counting chamber (Marienfeld).

FACS-based analyses

FACS analysis was performed on either a FACSARIA III cell sorter (BD Biosciences) or a FACSCalibur™ flow cytometer (BD Biosciences). In general, 2×10^7 parasites were washed, resuspended in PBS containing propidium iodide (PI) and incubated at room temperature for 10 min in the dark for PI exclusion assay for cell death analyses. The cells were subjected to FACS analysis ($ex\lambda = 488$ nm; $em\lambda = 617$ nm) using the FL2-H channel for PI analysis. Ten thousand events were analysed in each sample. To monitor GFP levels during GCV-negative selection or in GFP-LmaMPK4 transgenic parasites, parasites were analysed with the FL1-H channel for GFP fluorescence intensity ($ex\lambda = 395$ nm; $em\lambda = 509$ nm). Lesion-derived parasites were also examined for their GFP fluorescence intensity. Briefly, the parasites were extracted from the lesion by aspiration and were transferred to liquid media at 26°C for two passages to allow promastigote differentiation for further GFP levels evaluation. For metacyclic morphology analysis, cells were monitored using FSC/SSC dot plots. The raw data were acquired with CellQuest Pro 4.0 (BD Biosciences) and analysed using FlowJo 8.7 (Tree Star).

Metacyclic enrichment

(i) PNA agglutination. Parasites were purified as described previously (Sacks *et al*., 1985). Metacyclic parasites were collected from culture suspended at 2×10^6 parasites ml^{-1} at pH 7.4 or adjusted at pH 5.5 after 4 days of stationary growth. A total of 2×10^8 parasites ml^{-1} were incubated for 30 min at room temperature with 50 μg ml^{-1} peanut agglutinin (PNA) (Vector Labs) in M199 without serum. Agglutinated parasites were then removed by centrifugation for 10 min at 120 *g* and PNA(–) parasites were recovered from the supernatant by centrifugation for 10 min at 2500 *g*. The pellet was resuspended in incomplete culture medium, centrifuged under the same conditions and washed two times in incomplete medium. Parasites were counted using Neubauer counting chamber.

(ii) Ficoll gradient enrichment. Parasites were purified as described previously (Spath and Beverley, 2001). Briefly, a 20% stock solution of Ficoll type 400 (GE Healthcare) was prepared in sterile, endotoxin-free water filtered through a 0.22 μm cellulose acetate filter and kept at 4°C in darkness for no longer than 1 month. Working dilutions were prepared on the day that they were used. We used 15 ml Falcon conical centrifuge tubes containing 2 ml of Ficoll 20% overlaid by 2 ml of 10% Ficoll at the bottom, overlaid by 2 ml of M199 medium containing stationary growth phase parasites (2×10^8 cells ml^{-1}). These step gradients were centrifuged for 10 min at 1300 *g* at room temperature, and parasites were recovered from the interface with a sterile Pasteur pipette. Parasite fractions were washed once in 10 ml M199 medium by centrifugation. Those parasites were used for macrophages infection.

Macrophage infection

Peritoneal exudate macrophages (PEMs) were obtained from 6- to 8-week-old female BALB/c mice (Charles River Breeding Laboratories) and were plated overnight in 24-well tissue culture plates containing 12 mm^2 coverslips at a density of 10^5 cells/coverslip. Cells were incubated at 37°C and 5% CO_2 in complete Dulbecco's modified Eagle's medium (DMEM) supplemented with 10% heat-inactivated fetal bovine serum (FBS) (HyClone, Thermo Scientific), 10 mM HEPES pH 7.4, 1 μM β-mercaptoethanol, 1 mM sodium pyruvate, 50 U ml^{-1} penicillin and 50 mg ml^{-1} streptomycin. Metacyclic-enriched parasite fractions obtained by Ficoll purification (see above) after growth for one passage in M199 at pH 5.5 to induce metacyclogenesis (Zakai *et al*., 1998) were used to infect PEMs at 34°C for 4 h in DMEM-0.7% bovine serum albumin (BSA) using a parasites/macrophages ratio of 10:1 or 5:1. Non-internalized parasites were removed by repeated washing and cultures were further incubated at 34°C and 5% CO_2. Infection efficiency and intracellular parasite burden were assessed at day 0, 1, 2, 3 and 6 or at 0, 1, 2 and 5 by microscopic examination of infected cells after Hoechst (Hoechst 33342) staining (Spath *et al*., 2000).

Mouse infections

Parasite virulence was assessed by footpad analysis as described previously (Titus *et al*., 1991). Groups of six BALB/c mice were injected subcutaneously with 5×10^5 PNA-enriched parasites resuspended in 50 μl of PBS in the left hind footpad. We monitored lesion development by measuring the thickness of the footpad with a Vernier caliper.

Ethics statement

All animals were housed in our A3 animal facilities in compliance with the guidelines of the A3 animal facilities at the Pasteur Institute, which is a member of Committee 1 of the 'Comité d'Ethique pour l'Expérimentation Animale' (CEEA) – Ile de France – Animal housing conditions and the protocols used in the work described herein were approved by the 'Direction des Transports et de la Protection du Public, Sous-Direction de la Protection Sanitaire et de l'Environnement, Police Sanitaire des Animaux under numbers B75-15-27 and B75-15-28 in accordance with the Ethics Charter of animal experimentation that includes appropriate procedures to minimize pain and animal suffering. GS is authorized to perform experiment on vertebrate animals (licence B75-1159) issued

by the 'Direction Départementale de la Protection des Populations de Paris' and is responsible for all the experiments conducted personally or under his supervision as governed by the laws and regulations relating to the protection of animals.

Acknowledgements

We thank the members of the ParSig Unit for critical reading of the manuscript, Sophie Veillault for editorial help, and Stephen Beverley, Washington University School of Medicine, St. Louis, MO, USA for providing the pXNG vector. We thank Pierre-Henri Commere for expert assistance in FACS sorting. We thank Martin Wiese, Strathclyde Institute of Pharmacy and Biomedical Sciences, Glasgow, UK, for providing recombinant WT and dead mutant LmxMPK4. This work was supported by the 7th Framework Programme of the European Community through a grant to the LEISHDRUG (223414) consortium, by the Agence Nationale de Recherche through a grant to the ANR-11-RPIB-0016 TRANSLEISH consortium, and the French Government's Investissements d'Avenir programme: Laboratoire d'Excellence 'Integrative Biology of Emerging Infectious Diseases' (Grant No. ANR-10-LABX-62-IBEID). MD was the recipient of a Bourse de stage from the International Division of the Pasteur Institut and of a Bourse Fin de these scientifique from the Fondation de Recherche Médicale Equipe FRM programme (FDT20110922563).

References

Agron, P.G., Reed, S.L., and Engel, J.N. (2005) An essential, putative MEK kinase of *Leishmania major*. *Mol Biochem Parasitol* **142:** 121–125.

Apweiler, R., Bairoch, A., and Wu, C.H. (2004) Protein sequence databases. *Curr Opin Chem Biol* **8:** 76–80.

Aslett, M., Aurrecoechea, C., Berriman, M., Brestelli, J., Brunk, B.P., Carrington, M., *et al*. (2010) TriTrypDB: a functional genomic resource for the Trypanosomatidae. *Nucleic Acids Res* **38:** D457–D462.

Bao, Y., Weiss, L.M., Ma, Y.F., Lisanti, M.P., Tanowitz, H.B., Das, B.C., *et al*. (2010) Molecular cloning and characterization of mitogen-activated protein kinase 2 in *Trypanosoma cruzi*. *Cell Cycle* **9:** 2888–2896.

Bastin, P., Ellis, K., Kohl, L., and Gull, K. (2000) Flagellum ontogeny in trypanosomes studied via an inherited and regulated RNA interference system. *J Cell Sci* **113** (Part 18): 3321–3328.

Bates, P.A., and Tetley, L. (1993) *Leishmania mexicana*: induction of metacyclogenesis by cultivation of promastigotes at acidic pH. *Exp Parasitol* **76:** 412–423.

Bengs, F., Scholz, A., Kuhn, D., and Wiese, M. (2005) LmxMPK9, a mitogen-activated protein kinase homologue affects flagellar length in *Leishmania mexicana*. *Mol Microbiol* **55:** 1606–1615.

Carrera, A.C., Alexandrov, K., and Roberts, T.M. (1993) The conserved lysine of the catalytic domain of protein kinases is actively involved in the phosphotransfer reaction and not required for anchoring ATP. *Proc Natl Acad Sci USA* **90:** 442–446.

Chang, L., and Karin, M. (2001) Mammalian MAP kinase signalling cascades. *Nature* **410:** 37–40.

Croft, S.L., and Coombs, G.H. (2003) Leishmaniasis – current chemotherapy and recent advances in the search for novel drugs. *Trends Parasitol* **19:** 502–508.

Cunningham, M.L., Titus, R.G., Turco, S.J., and Beverley, S.M. (2001) Regulation of differentiation to the infective stage of the protozoan parasite *Leishmania major* by tetrahydrobiopterin. *Science* **292:** 285–287.

Desjeux, P. (2004) Leishmaniasis: current situation and new perspectives. *Comp Immunol Microbiol Infect Dis* **27:** 305–318.

Domenicali Pfister, D., Burkard, G., Morand, S., Renggli, C.K., Roditi, I., and Vassella, E. (2006) A mitogen-activated protein kinase controls differentiation of bloodstream forms of *Trypanosoma brucei*. *Eukaryot Cell* **5:** 1126–1135.

Dorin-Semblat, D., Quashie, N., Halbert, J., Sicard, A., Doerig, C., Peat, E., *et al*. (2007) Functional characterization of both MAP kinases of the human malaria parasite *Plasmodium falciparum* by reverse genetics. *Mol Microbiol* **65:** 1170–1180.

Dujardin, J.C., Gonzalez-Pacanowska, D., Croft, S.L., Olesen, O.F., and Spath, G.F. (2010) Collaborative actions in anti-trypanosomatid chemotherapy with partners from disease endemic areas. *Trends Parasitol* **26:** 395–403.

Erdmann, M., Scholz, A., Melzer, I.M., Schmetz, C., and Wiese, M. (2006) Interacting protein kinases involved in the regulation of flagellar length. *Mol Biol Cell* **17:** 2035–2045.

Feng, X., Rodriguez-Contreras, D., Polley, T., Lye, L.F., Scott, D., Burchmore, R.J., *et al*. (2013) 'Transient' genetic suppression facilitates generation of hexose transporter null mutants in *Leishmania mexicana*. *Mol Microbiol* **87:** 412–429.

Ghedin, E., Charest, H., Zhang, W.W., Debrabant, A., Dwyer, D., and Matlashewski, G. (1998) Inducible expression of suicide genes in *Leishmania donovani* amastigotes. *J Biol Chem* **273:** 22997–23003.

Ghosh, A.K., Bhattacharyya, F.K., and Ghosh, D.K. (1985) *Leishmania donovani*: amastigote inhibition and mode of action of berberine. *Exp Parasitol* **60:** 404–413.

Gupta, C.L., Khan, M.K., Khan, M.F., and Tiwari, A.K. (2013) Homology modeling of LmxMPK4 of *Leishmania mexicana* and virtual screening of potent inhibitors against it. *Interdiscip Sci* **5:** 136–144.

Hassan, P., Fergusson, D., Grant, K.M., and Mottram, J.C. (2001) The CRK3 protein kinase is essential for cell cycle progression of *Leishmania mexicana*. *Mol Biochem Parasitol* **113:** 189–198.

Hertz-Fowler, C., Peacock, C.S., Wood, V., Aslett, M., Kerhornou, A., Mooney, P., *et al*. (2004) GeneDB: a resource for prokaryotic and eukaryotic organisms. *Nucleic Acids Res* **32:** D339–D343.

Horjales, S., Schmidt-Arras, D., Limardo, R.R., Leclercq, O., Obal, G., Prina, E., *et al*. (2012) The crystal structure of the MAP kinase LmaMPK10 from *Leishmania major* reveals parasite-specific features and regulatory mechanisms. *Structure* **20:** 1649–1660.

John von Freyend, S., Rosenqvist, H., Fink, A., Melzer, I.M., Clos, J., Jensen, O.N., *et al*. (2010) LmxMPK4, an essential mitogen-activated protein kinase of *Leishmania mexicana* is phosphorylated and activated by the STE7-like protein kinase LmxMKK5. *Int J Parasitol* **40:** 969–978.

Kapler, G.M., Coburn, C.M., and Beverley, S.M. (1990) Stable transfection of the human parasite *Leishmania major* delineates a 30-kilobase region sufficient for extrachromosomal replication and expression. *Mol Cell Biol* **10:** 1084–1094.

Kultz, D. (1998) Phylogenetic and functional classification of mitogen- and stress-activated protein kinases. *J Mol Evol* **46:** 571–588.

LeBowitz, J.H. (1994) Transfection experiments with *Leishmania*. *Methods Cell Biol* **45:** 65–78.

Morales, M.A., Renaud, O., Faigle, W., Shorte, S.L., and Spath, G.F. (2007) Over-expression of *Leishmania major* MAP kinases reveals stage-specific induction of phosphotransferase activity. *Int J Parasitol* **37:** 1187–1199.

Morales, M.A., Pescher, P., and Spath, G.F. (2010a) *Leishmania major* MPK7 protein kinase activity inhibits intracellular growth of the pathogenic amastigote stage. *Eukaryot Cell* **9:** 22–30.

Morales, M.A., Watanabe, R., Dacher, M., Chafey, P., Osorio y Fortea, J., Scott, D.A., *et al*. (2010b) Phosphoproteome dynamics reveal heat-shock protein complexes specific to the *Leishmania donovani* infectious stage. *Proc Natl Acad Sci USA* **107:** 8381–8386.

Mottram, J.C., McCready, B.P., Brown, K.G., and Grant, K.M. (1996) Gene disruptions indicate an essential function for the LmmCRK1 cdc2-related kinase of *Leishmania mexicana*. *Mol Microbiol* **22:** 573–583.

Mukherjee, A., Roy, G., Guimond, C., and Ouellette, M. (2009) The gamma-glutamylcysteine synthetase gene of *Leishmania* is essential and involved in response to oxidants. *Mol Microbiol* **74:** 914–927.

Muller, I.B., Domenicali-Pfister, D., Roditi, I., and Vassella, E. (2002) Stage-specific requirement of a mitogen-activated protein kinase by *Trypanosoma brucei*. *Mol Biol Cell* **13:** 3787–3799.

Murta, S.M., Vickers, T.J., Scott, D.A., and Beverley, S.M. (2009) Methylene tetrahydrofolate dehydrogenase/cyclohydrolase and the synthesis of 10-CHO-THF are essential in *Leishmania major*. *Mol Microbiol* **71:** 1386–1401.

Muyombwe, A., Olivier, M., Ouellette, M., and Papadopoulou, B. (1997) Selective killing of *Leishmania* amastigotes expressing a thymidine kinase suicide gene. *Exp Parasitol* **85:** 35–42.

Naula, C., Parsons, M., and Mottram, J.C. (2005) Protein kinases as drug targets in trypanosomes and *Leishmania*. *Biochim Biophys Acta* **1754:** 151–159.

Ngo, H., Tschudi, C., Gull, K., and Ullu, E. (1998) Double-stranded RNA induces mRNA degradation in *Trypanosoma brucei*. *Proc Natl Acad Sci USA* **95:** 14687–14692.

Ojo, K.K., Arakaki, T.L., Napuli, A.J., Inampudi, K.K., Keyloun, K.R., Zhang, L., *et al*. (2011) Structure determination of glycogen synthase kinase-3 from *Leishmania major* and comparative inhibitor structure-activity relationships with *Trypanosoma brucei* GSK-3. *Mol Biochem Parasitol* **176:** 98–108.

Pearson, G., Robinson, F., Beers Gibson, T., Xu, B.E., Karandikar, M., Berman, K., *et al*. (2001) Mitogen-activated protein (MAP) kinase pathways: regulation and physiological functions. *Endocr Rev* **22:** 153–183.

Pfaffl, M.W. (2001) A new mathematical model for relative quantification in real-time RT-PCR. *Nucleic Acids Res* **29:** e45.

Posada, J., and Cooper, J.A. (1992) Requirements for phosphorylation of MAP kinase during meiosis in Xenopus oocytes. *Science* **255:** 212–215.

Prina, E., Roux, E., Mattei, D., and Milon, G. (2007) *Leishmania* DNA is rapidly degraded following parasite death: an analysis by microscopy and real-time PCR. *Microbes Infect* **9:** 1307–1315.

Rangarajan, R., Bei, A.K., Jethwaney, D., Maldonado, P., Dorin, D., Sultan, A.A., *et al*. (2005) A mitogen-activated protein kinase regulates male gametogenesis and transmission of the malaria parasite *Plasmodium berghei*. *EMBO Rep* **6:** 464–469.

Robbins, D.J., Zhen, E., Owaki, H., Vanderbilt, C.A., Ebert, D., Geppert, T.D., *et al*. (1993) Regulation and properties of extracellular signal-regulated protein kinases 1 and 2 *in vitro*. *J Biol Chem* **268:** 5097–5106.

Robinson, M.J., Harkins, P.C., Zhang, J., Baer, R., Haycock, J.W., Cobb, M.H., *et al*. (1996) Mutation of position 52 in ERK2 creates a nonproductive binding mode for adenosine 5′-triphosphate. *Biochemistry* **35:** 5641–5646.

Roskoski, R., Jr (2012) ERK1/2 MAP kinases: structure, function, and regulation. *Pharmacol Res* **66:** 105–143.

Sacks, D.L., and Perkins, P.V. (1984) Identification of an infective stage of *Leishmania* promastigotes. *Science* **223:** 1417–1419.

Sacks, D.L., Hieny, S., and Sher, A. (1985) Identification of cell surface carbohydrate and antigenic changes between noninfective and infective developmental stages of *Leishmania major* promastigotes. *J Immunol* **135:** 564–569.

Saravanan, P., Venkatesan, S.K., Mohan, C.G., Patra, S., and Dubey, V.K. (2010) Mitogen-activated protein kinase 4 of *Leishmania* parasite as a therapeutic target. *Eur J Med Chem* **45:** 5662–5670.

Schmidt-Arras, D., Leclercq, O., Gherardini, P.F., Helmer-Citterich, M., Faigle, W., Loew, D., *et al*. (2011) Adaptation of a 2D in-gel kinase assay to trace phosphotransferase activities in the human pathogen *Leishmania donovani*. *J Proteomics* **74:** 1644–1651.

Shi, H., Djikeng, A., Mark, T., Wirtz, E., Tschudi, C., and Ullu, E. (2000) Genetic interference in *Trypanosoma brucei* by heritable and inducible double-stranded RNA. *RNA* **6:** 1069–1076.

Spath, G.F., and Beverley, S.M. (2001) A lipophosphoglycan-independent method for isolation of infective *Leishmania* metacyclic promastigotes by density gradient centrifugation. *Exp Parasitol* **99:** 97–103.

Spath, G.F., Epstein, L., Leader, B., Singer, S.M., Avila, H.A., Turco, S.J., *et al*. (2000) Lipophosphoglycan is a virulence factor distinct from related glycoconjugates in the protozoan parasite *Leishmania major*. *Proc Natl Acad Sci USA* **97:** 9258–9263.

Titus, R.G., Muller, I., Kimsey, P., Cerny, A., Behin, R., Zinkernagel, R.M., *et al*. (1991) Exacerbation of experimental murine cutaneous leishmaniasis with CD4+ *Leishmania major*-specific T cell lines or clones which secrete interferon-gamma and mediate parasite-specific delayed-type hypersensitivity. *Eur J Immunol* **21:** 559–567.

Vergnes, B., Sereno, D., Tavares, J., Cordeiro-da-Silva, A., Vanhille, L., Madjidian-Sereno, N., *et al*. (2005) Targeted

disruption of cytosolic SIR2 deacetylase discloses its essential role in *Leishmania* survival and proliferation. *Gene* **363:** 85–96.

Wang, Q., Melzer, I.M., Kruse, M., Sander-Juelch, C., and Wiese, M. (2005) LmxMPK4, a mitogen-activated protein (MAP) kinase homologue essential for promastigotes and amastigotes of *Leishmania mexicana*. *Kinetoplastid Biol Dis* **4:** 6.

Wiese, M. (1998) A mitogen-activated protein (MAP) kinase homologue of *Leishmania mexicana* is essential for parasite survival in the infected host. *EMBO J* **17:** 2619–2628.

Wiese, M. (2007) *Leishmania* MAP kinases – familiar proteins in an unusual context. *Int J Parasitol* **37:** 1053–1062.

Wiese, M., Morris, A., and Grant, K.M. (2009) Trypanosomatid protein kinases as potential drug targets. In *Antiparasitic and Antibacterial Drug Discovery: From Molecular Targets to Drug Candidates*. Selzer, P.M. (ed.). Weinheim, Germany: Wiley-VCH Verlag GmbH & Co. KGaA, pp. 227–247.

Yan, C., Luo, H., Lee, J.D., Abe, J., and Berk, B.C. (2001) Molecular cloning of mouse ERK5/BMK1 splice variants and characterization of ERK5 functional domains. *J Biol Chem* **276:** 10870–10878.

Zakai, H.A., Chance, M.L., and Bates, P.A. (1998) *In vitro* stimulation of metacyclogenesis in *Leishmania braziliensis*, *L. donovani*, *L. major* and *L. mexicana*. *Parasitology* **116** (Part 4): 305–309.

Zilberstein, D., and Shapira, M. (1994) The role of pH and temperature in the development of *Leishmania* parasites. *Annu Rev Microbiol* **48:** 449–470.

Supporting information

Additional supporting information may be found in the online version of this article at the publisher's web-site.